CAPITAL UNIVERSITY OF SCIENCE AND TECHNOLOGY, ISLAMABAD

Effects of Mercaptobenzothiazole Derivative on Neuro-inflammatory Pain in Animal Models

by

Iqra Nawaz

A thesis submitted in partial fulfillment for the degree of Master of Philosophy

in the

Faculty of Pharmacy
Department of Pharmacology

2025

Dedicated to my parents, whose endless love and sacrifices shaped my journey and to those who guided and supported me with unwavering faith and kindness.

CERTIFICATE OF APPROVAL

Effects of Mercaptobenzothiazole Derivative on Neuro-inflammatory Pain in Animal Models

by

Iqra Nawaz

(MPH233007)

THESIS EXAMINING COMMITTEE

S. No.	Examiner	Name	Organization
(a)	External Examiner	Dr. Muhammad Faheem	RIU, Islamabad
(b)	Internal Examiner	Dr. Fazlullah Khan	CUST, Islamabad
(c)	Supervisor	Dr. Muzaffar Abbas	CUST, Islamabad

Dr. Muzaffar Abbas
Thesis Supervisor
October, 2025

Dr. Fazlullah Khan
Head
Department of Pharmacology
October, 2025

Dr. Muzaffar Abbas
Dean
Faculty of Pharmacy
October, 2025

Author's Declaration

I, **Iqra Nawaz** hereby state that my MPhil thesis titled "**Effects of Mercapto-benzothiazole Derivative on Neuro-inflammatory Pain in Animal Models**" is my own work and has not been submitted previously by me for taking any degree from Capital University of Science and Technology, Islamabad or anywhere else in the country/abroad.

At any time if my statement is found to be incorrect even after my graduation, the University has the right to withdraw my MPhil Degree.

(Iqra Nawaz)

Registration No: MPH233007

Plagiarism Undertaking

I solemnly declare that research work presented in this thesis titled "**Effects of Mercaptobenzothiazole Derivative on Neuro-inflammatory Pain in Animal Models**" is solely my research work with no significant contribution from any other person. Small contribution/help wherever taken has been duly acknowledged and that complete thesis has been written by me.

I understand the zero tolerance policy of the HEC and Capital University of Science and Technology towards plagiarism. Therefore, I as an author of the above titled thesis declare that no portion of my thesis has been plagiarized and any material used as reference is properly referred/cited.

I undertake that if I am found guilty of any formal plagiarism in the above titled thesis even after award of MPhil Degree, the University reserves the right to withdraw/revoke my MPhil degree and that HEC and the University have the right to publish my name on the HEC/University website on which names of students are placed who submitted plagiarized work.

(Iqra Nawaz)

Registration No: MPH233007

Acknowledgement

First and foremost, I bow in humble gratitude to Allah Almighty, whose infinite mercy, blessings, and guidance have illuminated every step of my journey. Without His divine support, none of this would have been possible.

This work is lovingly dedicated to my beloved father, Nawaz Shaheen (late), whose wisdom and strength continue to guide me. His memory inspires me every day to persevere and live a life he would be proud of. To my dearest mother Shahnaz Shaheen, your love is the most selfless gift I've ever known. Your prayers protected me, your courage inspired me, and your sacrifices made everything possible.

To my honorable supervisor, Dr. Muzaffar Abbas, PROFESSOR / DEAN FACULTY OF PHARMACY, no words can truly capture my gratitude for your role in my life. You are not only the finest mentor but the best person I have ever met. Your kindness, sincerity, and dedication to your students are unparalleled. Your loyalty to your profession, tireless hard work, and constant encouragement have left a lasting impact on me. I consider it a great privilege to have worked under your guidance.

To my beloved siblings Sehrish Nawaz, Rimsha Nawaz, Misbah Nawaz, Bushra Nawaz, Urooj Nawaz, and Noor-ul-Eman thank you for your endless love, support, and belief in me. To my dear brother, Muhammad Ali Nawaz, your quiet motivation and presence have been a steady support through every high and low. Thank you for always standing by me.

To my dear aunt Rehana Yasmeen, for her constant love, care, and all the thoughtful things she did for me throughout this journey. To my dear friends and colleagues Ms. Aqeela, Khurshid, Ms. Tuba Naseer, Ms. Sadia Khaliq, Ms. Noor-ul-Ain, Ms. Ibtisam Zakir and Ms. Anosh Khaliq thank you for your love, encouragement, and the many shared moments that carried me through the challenges and triumphs of this path. I would also like to thank Mr. Salaar Khan for his consistent and insightful suggestions during the course of this research.

To my respected seniors, Ms. Iqra Zulfiqar and Mr. M. Ibrar Khan your guidance and support have been a true blessing in my academic path.

I extend my heartfelt thanks to the faculty of the Department of Pharmacy, for their valuable guidance and support. This thesis reflects the contributions of all who believed in me and helped shape my journey.

(Iqra Nawaz)

Abstract

Pain is a debilitating condition that persists beyond normal healing and arises from sustained inflammation within the nervous system. Despite the availability of conventional therapies including nonsteroidal anti-inflammatory drugs (NSAIDs), corticosteroids, and opioids, long-term pain management remains unsatisfactory due to limited efficacy and significant side effects such as gastrointestinal damage, cardiovascular risks, and dependency issues. These limitations highlight the urgent need for safer and more effective analgesic agents, especially those capable of targeting inflammatory mechanisms.

This study investigates the therapeutic potential of a mercaptobenzothiazole derivative, a novel compound synthesized for its predicted neuroinflammatory properties. Using a complete freund's adjuvant (CFA)-induced model of neuroinflammatory pain in male Balb/C mice, the MBT derivative was evaluated for its efficacy in reducing both nociceptive behavior and neuroinflammation. Mice were divided into five groups: vehicle control, CFA-induced negative control, standard treatment (diclofenac, 5 mg/kg), and two MBT derivative treatment groups (5 mg/kg or 10 mg/kg).

Behavioral assessments including hot plate latency, von frey filament testing, and paw edema measurements were performed daily. Results demonstrated that MBT derivative at 10 mg/kg significantly alleviated thermal hyperalgesia, mechanical allodynia, and paw swelling compared to the negative control. The effect was dose-dependent, with the higher dose offering superior therapeutic outcomes.

Acute gross safety profile through an acute toxicity study (100 mg/kg) showed no signs of toxicity or behavioral abnormalities. *In silico* analysis, including molecular docking, revealed strong binding affinities with pro-inflammatory targets such as TNF-α, along with favorable ADME properties, supported the compound's mechanism of action and drug-likeness.

Taken together, these findings suggest that mercaptobenzothiazole derivative could be promising drug candidate for neuroinflammatory pain with improved efficacy and safety.

Contents

List of Figures

List of Tables

Abbreviations

ADME	Absorption, Distribution, Metabolism, and Excretion
AGD	Anogenital distance
BBB	Blood-Brain Barrier
BDNF	Brain-Derived Neurotrophic Factor
BCA	Bicinchoninic Acid
CCI	Chronic Constriction Injury
CFA	Complete Freund's adjuvant
CGRP	Calcitonin Gene-Related Peptide
CNS	Central Nervous System
CYP	Cytochrome P450 enzymes
ELISA	Enzyme-Linked Immunosorbent Assay
GI	Gastrointestinal
H&E	Hematoxylin and Eosin
IL-1β	Interleukin-1 β
IL-6	Interleukin-6
i.p	Intraperitoneal
JNK	Jun N-terminal kinase
LC	Locus Coeruleus
LPS	Lipopolysaccharide
MBT	Mercaptobenzothiazole
NF-κB	Nuclear Factor kappa-light-chain-enhancer of activated B cells
NOX	NADPH Oxidase
NSAIDs	Nonsteroidal anti-inflammatory drugs
PAG	Periaqueductal Gray

PDB	Protein Data Bank
ProTox	ProTox-3.0 Toxicity Prediction Web Server
PDBQT	Protein Data Bank, Partial Charges & Torsions
PSL	Partial Sciatic Nerve Ligation
RNS	Reactive Nitrogen Species
ROS	Reactive Oxygen Species
RVM	Rostral Ventromedial Medulla
SNI	Spared Nerve Injury
SNL	Spinal Nerve Ligation
SEM	Standard Error of Mean
TNF-α	Tumor Necrosis Factor-alpha
TLC	Thin Layer Chromatography
TLR	Toll-Like Receptor

Symbols

μ**L**	Microliter
μ**g**	Microgram
mg	Milligram
kg	Kilogram
%	Percentage
$^{\circ}$**C**	Degrees Celsius
$\pm$	Plus-minus
$\rightarrow$	Indicates direction of process or transformation
$\downarrow$ / $\uparrow$	Decrease / Increase
i.p.	Intraperitoneal
$\mathbf{p < 0.05}$	Statistically significant
Δ	Change in value
$\pm$ **SEM**	Standard Error of Mean

Chapter 1

Introduction

1.1 Overview

Pain is a multifaceted experience involving both physical sensation and emotional response, typically arising from actual or threatened tissue damage, though it may also occur in the absence of a clear physical cause [1]. A 2022 global study found that 27.5% of adults had pain, with higher rates in women, older adults, and rural areas [2]. In 2021, the global burden of disease study reported that 453 million people had low back pain, affecting 8.6% of the working-age population [3]. Pain affects up to 53% of people in Europe and the U.S., making it the third leading global health issue after heart disease, stroke and cancer. It significantly impacts quality of life and adds major economic burden [4]. Pain affects more than 30% of the global population, making it a significant and growing public health concern. It not only diminishes the quality of life for millions of individuals but also imposes a heavy burden on healthcare systems across the world. Pain is now recognized as one of the leading causes of hospital admissions, long-term disability, and reduced workforce productivity, thereby contributing to substantial economic losses. The persistent and often debilitating nature of pain demands the development of more effective management strategies and therapeutic interventions, particularly for pain types associated with inflammation [5].

1.2 Types of Pain

Pain can be categorized into distinct types based on its underlying mechanisms. Inflammatory nociceptive pain typically arises from tissue injury or localized inflammation, driven by the release of chemical mediators that activate nociceptors. This type of pain can involve visceral structures, such as internal organs, or somatic tissues, including skin, muscle, and bone. In contrast, neuropathic pain results from direct injury or disease affecting the somatosensory nervous system. Common causes include nerve compression, trauma, exposure to neurotoxic agents (e.g., chemotherapeutic drugs), metabolic disorders like diabetes, viral infections, and autoimmune conditions, often mediated by complex immune signaling pathways.

A third category, nociplastic pain, is characterized by altered nociceptive processing in the absence of detectable tissue damage or identifiable pathology in the somatosensory system. Notably, many patients exhibit overlapping features of these pain types, which complicates accurate diagnosis and effective treatment [6].

1.3 Pain Pathways

Pain perception is a multifaceted process governed by intricate interactions between ascending and descending neural pathways. The mechanism begins with the activation of nociceptors, specialized sensory neurons located in the dorsal root ganglia, which extend peripherally to tissues and centrally to the dorsal horn of the spinal cord. These receptors respond by potentially harmful mechanical, thermal or chemical stimuli, and these receptors connect with two main types of nerve fibers that transmit pain signals to the spinal cord [7]. The first type, myelinated Aδ fibers, are covered with a myelin sheath, which allows them to conduct impulses rapidly and convey sensations of sharp, sudden, and well-defined pain, such as the immediate pain felt when pricked by a needle. In contrast, unmyelinated C fibers lack this myelin covering, resulting in slower conduction, and they carry signals of dull, aching, burning, or persistent pain, like the lingering discomfort experienced after an injury. In the dorsal horn, nociceptors fill excitatory neurotransmitters

such as glutamate, substance P, calcitonin-gene related peptides (CGRP) and brain derived neurotrophic factor (BDNF) to activate secondary projection neurons.

These neurons spread pain signals through elevated pathways to higher brain regions. At the same time, descending modulation systems derived from the periaqueductal grey (PAG), rostral ventromedial medulla (RVM), and locus coeruleus (LC) exercise bidirectional control for nociceptive spinal processing. These top down paths can inhibit or ameliorate dorsal horn pain signals through the release of neurotransmitters to allow for adaptive modulation of pain perception based on contextual factors, emotional conditions, and previous experience [8].

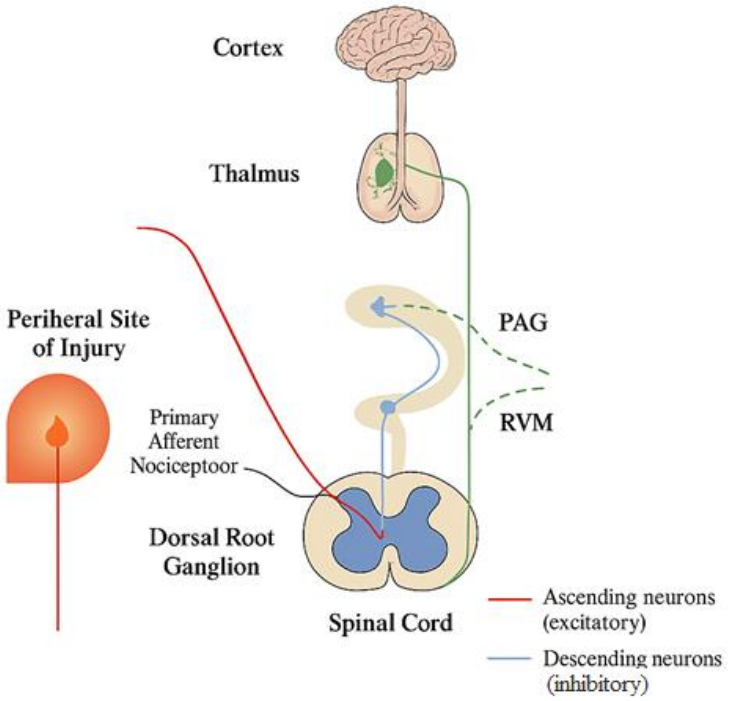

FIGURE 1.1: Schematic representations of ascending and descending pain

The above figure demonstrates the basic organization of the nociceptive signaling system. The ascending pathway (shown in red) begins at the peripheral site of injury, where nociceptors detect harmful stimuli. The signal travels via the dorsal root ganglion into the spinal cord, ascending through second order neurons to the thalamus, and ultimately reaching the cerebral cortex, where pain is consciously perceived. Conversely, the descending pathway (shown in green and blue) originates from the cortex and thalamus, projecting to midbrain regions like the periaqueductal gray (PAG) and the rostral ventromedial medulla (RVM) [9]. These structures send

descending inhibitory or excitatory signals back to the spinal cord, modulating pain transmission at the level of the dorsal horn.

Inflammatory pain, a type of pathological pain, arises in peripheral tissues and is commonly caused by factors like trauma, bacterial infections, or viral infections. It results from the immune system's reaction to these harmful stimuli, causing persistent activation of pain pathways and prolonged sensitivity in the affected regions. This condition is a significant global health issue. Among the various mechanisms driving pain, inflammation is central to the onset and persistence of many pain disorders [10]. Inflammation is a critical biological reaction to tissue injury or infection, marked by the activation of immune cells and the release of numerous inflammatory mediators. While inflammation is vital for tissue healing and protection against pathogens, its improper regulation can lead to adverse outcomes. When inflammation occurs within the nervous system, it can trigger a condition referred to as neuroinflammatory pain.

1.4 Neuroinflammatory Pain

Neuroinflammatory pain is a debilitating condition marked by sustained inflammation in neural tissues, which disrupts normal neuronal function and leads to persistent pain sensations. This maladaptive inflammatory state can be triggered by a range of factors, including nerve injury, autoimmune disorders, chronic infections, or metabolic diseases. Peripheral sensitization, involving increased responsiveness of nociceptive neurons at the site of injury, primarily initiates the pain process. In contrast, central sensitization characterized by the amplification of pain signals within the spinal cord and brain plays a critical role in the maintenance and chronicity of pain, even after the original injury has resolved [11]. The complex interplay of these mechanisms results in heightened pain perception and spontaneous pain. Furthermore, the activation of glial cells, such as astrocytes and microglia, along with peripheral immune cells like neutrophils, macrophages, T-cells, and mast cells, contributes significantly to the initiation and persistence of Neuroinflammatory pain [12]. These cells release a variety of inflammatory cytokines, chemokines and

neuroactive substances that regulate neuronal excitability and synaptic transmission and thus maintain pain. Understanding cellular and molecular mechanisms based on neuroinflammation is essential for developing new therapeutic strategies to alleviate these pain conditions [13, 14]. However, if this protective response is dysregulated or expanded, it may contribute to the pathogenesis of pain, which underscores the importance of understanding the underlying mechanism.

Though its role as a defense mechanism, inflammation causes a cascade of physiological changes to reduce further damage and neutralize potentially harmful pathogens. This process involves a coordinated sequence of cellular events, such as targeted movement of leukocytes in the direction of the affected area, and release of vasoactive effects. These responses not only serve to isolate and contain the injury but also provide the necessary components for tissue repair. However, when the inflammatory response becomes unremitting, it transitions from a protective process to a pathological one [15]. Inflammation is implicated in the progression of several serious conditions such as psoriasis, multiple sclerosis, and rheumatoid arthritis where sustained immune activation leads to structural and functional damage of tissues and organs. The ongoing presence of inflammatory mediators in these diseases often results in progressive deterioration, increasing both morbidity and the risk of mortality. The detrimental effects of this long-term inflammatory state highlight the urgent need for improved diagnostic, management and treatment strategies aimed at restoring the balance of the immune system and maintaining organ function [16]. Proinflammatory mediators such as interleukin-1 β, tumor necrosis factor alpha (TNF-alpha), and nitrogen oxides play a central role in regulating pain during inflammation. In the event of tissue damage or infection, these substances are released immediately into the region environment, where they interact with specific receptors expressed in nociceptive neurons. This binding initiates an intracellular signal cascade that increases the sensitivity of these neurons, leading to peripheral sensitization, which can result in benign stimuli that usually cause painful sensations. In addition to sensitization of neurons within affected tissues, these mediators also contribute to central sensitization. It strengthens the signal of pain transmitted along the ascending pathway by modulating synaptic transmission and neural circuit plasticity within the spinal cord [17]. This dual mechanism improves the sensitivity of both the peripheral region and the central processing center to the

feedback loop that enhances the chronic pain. As a result, the persistent effects of IL-1, TNF-alpha, and nitrogen oxides not only increase immediate pain responses, but also lie in the basis of long-term changes in neural function associated with pain disorders [18]. These chronic pain conditions represent a growing global health challenge with far-reaching implications beyond individual suffering.

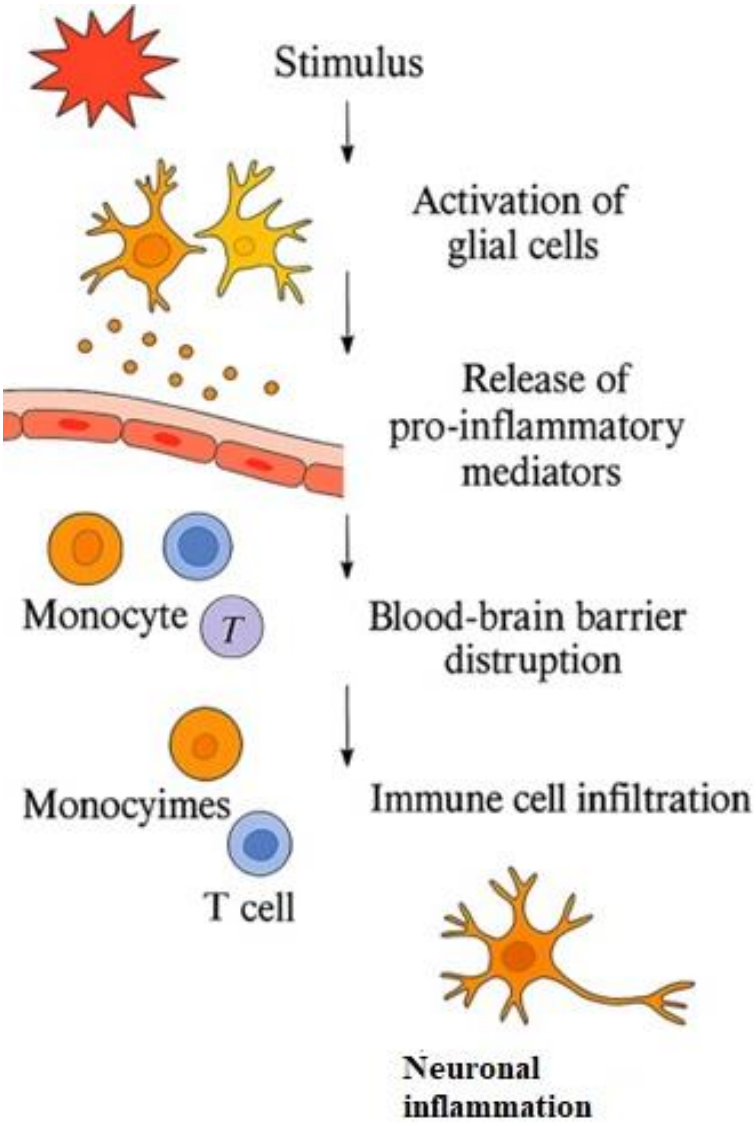

FIGURE 1.2: Mechanism of neuroinflammation leading to neuronal damage

The above diagram illustrates the sequential cellular and molecular events in neuroinflammation, beginning from an external stimulus to neuronal injury. Key features include glial activation, release of pro-inflammatory mediators, blood-brain barrier (BBB) disruption, infiltration of peripheral immune cells, and eventual neuronal degeneration

1.5 Current Pharmacological Approaches and their Limitations

Pain persists as a growing global health challenge, affecting a significant portion of the population. Despite the widespread use of existing pharmacologic agents, effective management of inflammatory pain remains a major unresolved challenge in modern medicine. NSAIDs have long been the cornerstone of treatment for mild to moderate inflammatory pain due to their ability to inhibit cyclooxygenase enzymes and reduce prostaglandin synthesis. However, their benefits are often outweighed by the significant risks associated with long-term use, such as gastrointestinal ulceration, bleeding, and an increased risk of cardiovascular events [19]. NSAIDs such as ibuprofen, naproxen, and COX-2 inhibitors provide effective analgesia and anti-inflammatory effects by inhibiting prostaglandin synthesis, but they carry significant risks when used chronically. These include gastrointestinal toxicity (ulcers, bleeding), renal impairment due to reduced renal perfusion and electrolyte disturbances, and heightened cardiovascular events such as hypertension, myocardial infarction, and exacerbation of heart failure, with COX-2 selective agents posing greater thromboembolic risk [20]. Acetaminophen, while safer on the stomach, poses dose-dependent hepatotoxicity risks (>3 g/day) and minor cardiovascular/renal effects [21]. In cases of more severe pain, opioid analgesics are frequently employed, yet these drugs present their own array of complications including the development of tolerance, physical dependence, and a heightened risk of misuse and addiction. Moreover, while opioids are effective in providing temporary relief, they do little to address the underlying inflammatory processes that perpetuate the pain state. This shortfall highlights a critical therapeutic void in the existing pain management arsenal. The persistent inadequacy of current treatment options has spurred ongoing research efforts aimed at uncovering novel molecular targets and signaling pathways that drive inflammatory pain [22]. Opioids containing codeine, morphine, tramadol and fentanyl activate opioid receptors to relieve moderately severe pain, but are limited by side effects such as sedation, respiratory depression, constipation, immunosuppression, hormonal changes, and paratoxic hypertrophy. Long-term use leads to tolerance and addiction that

promotes public health crisis [23]. Antidepressants such as amitriptyline and duloxetine demonstrate therapeutic efficacy in managing neuropathic pain conditions. However, their clinical use may be associated with several adverse effects, including central nervous system depression (sedation), anticholinergic effects (dry mouth), postural hypotension (dizziness), metabolic alterations (weight gain), peripheral fluid retention (edema), cognitive impairment, cardiac conduction abnormalities (arrhythmias), and sexual dysfunction [24].

Anticonvulsant medications such as gabapentin and pregabalin demonstrate efficacy in managing neuroinflammatory pain conditions. However, their therapeutic use may be accompanied by adverse effects including dizziness, sedation, peripheral edema, and increased body weight. In uncommon cases, these agents have been associated with more serious complications such as respiratory suppression, alterations in mood, or discontinuation symptoms upon abrupt cessation [25].

However, prolonged administration or higher dosages are constrained by undesirable effects such as marked immune suppression, bone density loss, elevated blood sugar levels and impaired glucose metabolism, neuropsychiatric complications (including affective disorders and drug-induced psychotic symptoms), and disruptions in metabolic homeostasis [26].

Corticosteroids, including dexamethasone and prednisolone, are commonly prescribed for managing neuroinflammatory conditions. However, their therapeutic use is accompanied by considerable adverse effects, including compromised immune function, elevated blood glucose levels, increased blood pressure, reduced bone mineral density, neuropsychiatric alterations, and the development of Cushing's syndrome-like symptoms. These adverse effects limit their long-term use in clinical settings [27].

1.6 Need for Novel Therapeutic Strategies

By exploring alternative mechanisms such as specific cytokine inhibitors, modulators of ion channels involved in nociception, or agents that directly target glial cell

activation researchers hope to develop therapies that not only alleviate pain more effectively but also offer a superior safety profile. Ultimately, advancing our understanding of the complex biological underpinnings of inflammatory pain is essential for the development of innovative pharmacological strategies that can break the cycle of pain and reduce the substantial clinical and economic burdens it imposes [28]. One promising direction in this pursuit involves exploring heterocyclic compounds with potent bioactivity, such as benzothiazole derivatives.

1.7 Benzothiazole as a Promising Scaffold in Drug Discovery

Benzothiazole is a highly significant heterocyclic compound that has gained remarkable attention in the fields of bioorganic and medicinal chemistry due to its broad range of biological and pharmacological activities. It is regarded as a privileged structure because it is often found in compounds with potent and diverse biological effects. Even though it possesses a relatively small and simple framework, benzothiazole exhibits remarkable versatility and has been extensively explored in drug discovery and development. The benzothiazole scaffold serves as a fundamental structural component in numerous pharmacologically active compounds, frequently contributing to enhanced drug efficacy and optimized therapeutic characteristics [29]. The benzothiazole molecular framework has shown diverse pharmacological potential, exhibiting antimicrobial, antitumor, antiparasitic, and hypoglycemic effects. These versatile properties have established benzothiazole derivatives as valuable candidates in contemporary drug discovery. Beyond therapeutic applications, these compounds play significant industrial roles, particularly as oxidation inhibitors and polymerization catalysts in rubber manufacturing processes. Particularly, derivatives like 2-aryl benzothiazoles have received widespread attention because of their unique structural attributes and specialized uses, such as in radioactive imaging for amyloid plaques linked to neurodegenerative diseases like alzheimer's. Furthermore, several 2-aminobenzothiazole derivatives have been intensively studied since the 1950s, as they possess enhanced cytotoxic effects

against cancer cells. These findings have spurred efforts to further optimize their structures for improved medicinal applications.

In medicinal chemistry the strategic combination of 2-aminobenzothiazole with other heterocyclic moieties has emerged as an important approach, allowing the development of novel drug candidates with modified pharmacological profiles, reduced toxicity, and improved efficacy. The benzothiazole core structure has emerged as a privileged scaffold in medicinal chemistry, particularly for developing novel therapeutics targeting multifactorial diseases involving inflammatory cascades, redox imbalances, and immune system dysfunction. This molecular framework demonstrates remarkable target, exhibiting modulatory effects on diverse biological macromolecules including catalytic proteins and cell surface receptors, which accounts for its broad pharmacological applicability. Due to their small size, lipophilicity, and capability to form hydrogen bonds and hydrophobic interactions, benzothiazole derivatives can effectively cross biological membranes, reaching their intracellular targets [30]. These characteristics prove especially valuable in developing treatments for neuroinflammatory disorders, where therapeutic agents require efficient blood-brain barrier permeability. Current investigations are progressively examining benzothiazole derivatives as promising candidates for managing neuroinflammatory pain and related neurological pathologies. Given its biological significance, structural simplicity, and pharmaceutical potential, benzothiazole continues to be a focal point in the search for new, effective therapies [31]. Structurally, benzothiazole consists of a benzene ring fused with a thiazole ring at the 4,5-positions, forming a bicyclic system. The thiazole moiety represents a five-membered heterocyclic structure comprising one sulfur atom and one nitrogen atom within its ring system. According to standard nomenclature conventions, the ring numbering system initiates at the sulfur position. This heterocyclic scaffold was first characterized by Hantzsch and Weber in 1887, with subsequent structural verification provided by Popp in 1889. Benzothiazole inherits the chemical characteristics of the thiazole ring while gaining additional stability and reactivity from the benzene moiety. This fused ring system imparts unique electronic and steric properties to benzothiazole, which are critical for its interaction with biological systems [32]. These distinctive chemical features make benzothiazole

derivatives promising candidates for a variety of therapeutic applications, including inflammation-related conditions.

In particular, benzothiazoles are a versatile class of bicyclic compounds that naturally occur in various sources and have been recognized for a wide range of biological activities, notably in the realm of anti-inflammatory effects. 2-mercaptobenzothiazole has emerged as a key structural motif with significant therapeutic potential in regulating inflammatory processes and managing pain.

Utilizing the benefits of click chemistry, renowned for its high efficiency, exceptional selectivity, and mild reaction conditions it was successfully synthesized an extensive array of novel bis-heterocyclic compounds.

This was achieved through the strategic conjugation of 2-mercaptobenzothiazole scaffolds with 1,2,3-triazole ring systems. This combinatorial approach not only allowed for the rapid generation of molecular diversity but also facilitated systematic exploration of structure activity relationships [33].

Preliminary pharmacological screening revealed that multiple synthesized derivatives exhibit significant anti-inflammatory and analgesic properties in preclinical models. Notably, select compounds demonstrated comparable efficacy to ibuprofen a benchmark NSAID commonly used in clinical practice as evidenced by standardized *in vivo* assays measuring inflammation reduction and pain threshold modulation. Remarkably, these novel agents achieved such significant pharmacological actions without inducing the gastrointestinal side effects specifically, gastric ulcers that are commonly associated with long-term NSAID therapy [34].

These results underscore the potential of 2-mercaptobenzothiazole-based bis-heterocycles as promising leads for the development of safer anti-inflammatory and analgesic drugs. Furthermore, the effective implementation of click chemistry in assembling these molecular architectures establishes a versatile platform for developing novel multifunctional therapeutics. This approach enables precise targeting of intricate pathological pathways involved in inflammatory processes and nociceptive signaling, thereby expanding opportunities for innovative drug discovery in pain and inflammation therapeutics [35].

1.8 Mechanistic Insights and Structural Optimization

Rational structural optimization of these compounds frequently enhances their chemical stability, metabolic resistance, and lipophilic character. Such molecular improvements typically translate to superior pharmacokinetic profiles, including enhanced bioavailability and improved blood-brain barrier permeability essential characteristics for therapeutics targeting neurological tissues in neuroinflammatory pain models.

Such modifications may enable derivatives to reach target sites in the central nervous system more effectively than their parent compounds [36]. Once at the target site, these structurally optimized compounds can exert their effects by modulating specific molecular pathways involved in neuroinflammation.

Research indicates that these compounds can inhibit key inflammatory enzymes and signaling pathways, such as c-Jun N-terminal kinases (JNKs), which are strongly associated with neuroinflammation. Structural modifications to the benzothiazole core can influence the electronic and steric characteristics of the molecule.

These changes may enhance interactions with biological targets, thereby potentially increasing the compound's anti-inflammatory potency [37]. One such strategic modification involves the incorporation of fluorine atoms, which has gained significant attention in medicinal chemistry.

The incorporation of fluorine into organic molecules is a well-established strategy in medicinal chemistry, aimed at enhancing the biological properties of compounds. Fluorine's unique characteristics, such as its high electronegativity and the exceptional strength of the carbon-fluorine bond, play a crucial role in altering the reactivity and stability of organic molecules.

Additionally, the lipophilicity imparted by fluorine substitution increases the solubility of such compounds in lipid membranes, which in turn improves their absorption, distribution, and interaction within biological systems [38]. These properties make

fluorine-containing molecules ideal candidates for drug development, as they often exhibit superior pharmacokinetic and pharmacodynamic profiles compared to their non-fluorinated counterparts. The strategic incorporation of fluorine substituents into thiadiazole-benzothiazole hybrid architectures represents a promising synthetic approach for developing novel therapeutics with optimized pharmacological properties [39].

This molecular design strategy capitalizes on the unique electronic effects of fluorine to enhance drug-like characteristics while maintaining the intrinsic biological activities of both heterocyclic systems. Benzothiazole scaffolds are particularly noted for their wide-ranging applications in pharmacology, including anti-inflammatory, antimicrobial, and anticancer activities. The addition of thiodizole further enriches the molecular structure by introducing additional functional groups that can interact favorably with biological targets. Together, these modifications hold the potential to develop novel drugs with improved efficacy, safety, and versatility across various therapeutic areas [40].

Such structural innovations contribute to the expanding utility of benzothiazole scaffolds in medicinal chemistry [41]. The addition of thiodizole further enriches the molecular structure by introducing additional functional groups that can interact favorably with biological targets. Collectively, these structural innovations may enable the development of next-generation therapeutics with enhanced pharmacological profiles, including greater target specificity, reduced adverse effects, and broader clinical applications across multiple disease indications [42].

1.9 Mechanism of Action – CFA-induced Inflammatory Pain

As shown in the above figure, CFA injection initiates a cascade of immune responses beginning with the activation of macrophages and neutrophils. This leads to the release of pro-inflammatory cytokines such as TNF-α, IL-1β, and IL-6. Subsequently, glial cell activation occurs within the spinal cord, contributing to central

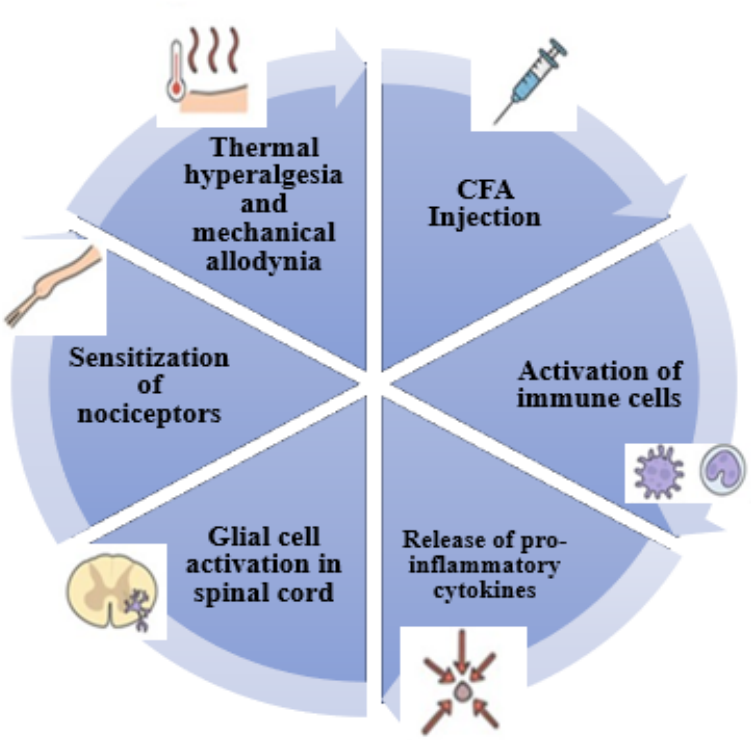

FIGURE 1.3: Schematic representation of the mechanism of action following CFA-induced inflammatory pain

sensitization. These events result in the sensitization of peripheral nociceptors, culminating in behavioral manifestations of thermal hyperalgesia and mechanical allodynia key features of Neuroinflammatory pain [43]. (Figure adapted from Lazarević et al., 2024).

1.9.1 Synthesis of MBT derivative

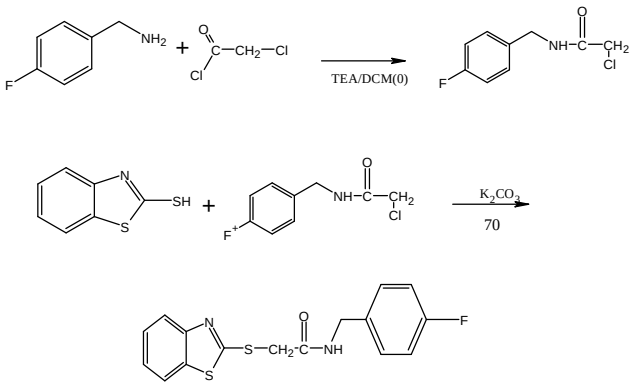

FIGURE 1.4: Synthesis pathway of fluorobenzylamine derivative conjugated with 2-mercaptobenzothiazole

The above reaction scheme illustrates the initial synthesis of fluorobenzylamine by reacting amines with chloroacetyl chloride in dichloromethane at 0°C in the presence of triethylamine, yielding amides after 4–5 hours. The amides were purified via standard workup and used in the subsequent reaction with 2-mercaptobenzothiazole in acetonitrile at 70°C using potassium carbonate as a base, with the reaction proceeding over 3–4 days to yield the final fluorobenzylamine–mercaptobenzothiazole derivative. Reaction progress was monitored using thin-layer chromatography (TLC) with a 1:1 petroleum ether and ethyl acetate mobile phase.

Initially fluoro benzylamine was synthesized by reacting amines with chloroacetyl chloride in the presence of triethylamine as a base and solvent used was dichloromethane, temperature should be maintained at zero degree. This reaction will take 4-5 hours to complete. The progress of reaction is monitored by doing TLC in 1:1 (Petroleum ether and ethyl acetate). After doing work up pure amides will be obtained which are further dried and used in next step for further reaction with 2-mercaptobenzothiazole. This reaction will take place in acetonitrile solvent, temperature should be maintained at 70 degree, base used was potassium carbonate and reaction take place in 3-4 days. After monitoring the progress of reaction by TLC in in 1:1 (Petroleum ether and ethyl acetate) the mixture with ethyl acetate and isolate pure product was extracted. [44, 45].

Chapter 2

Literature Review

Pain associated with inflammation, has long been a central focus of medical research due to its profound impact on health and quality of life. Researchers have dedicated extensive efforts to uncovering the molecular and cellular mechanisms behind inflammatory and neuroinflammatory pain to develop more effective treatments.

2.1 Mechanistic Insights into Pain Pathways

Julius and Basbaum in 2001 provided foundational insights into nociception, detailing how inflammatory mediators like prostaglandins and bradykinin sensitize peripheral nociceptors, triggering pain perception. Their work laid the groundwork for identifying key therapeutic targets [46]. Gereau and his colleagues in 2014 emphasized the complexity of pain, which involves not only peripheral nociceptor activation but also central sensitization, a phenomenon where the nervous system becomes hypersensitive to pain signals. They advocated for treatments that address these underlying mechanisms rather than merely alleviating symptoms [4]. Zhang and his colleagues in 2011 explored the role of glial cells (microglia and astrocytes) in neuroinflammatory pain, demonstrating that their activation leads to the release of pro-inflammatory cytokines (e.g., IL-1β, TNF-α), which amplify neuronal excitability and sustain chronic pain [12]. Ji and his colleagues., in 2006 expanded

on this by identifying NF-κB and JNK signaling pathways as critical drivers of glial activation, proposing that inhibiting these pathways could offer new therapeutic avenues [47]. Kobayashi and his colleagues in 2015 investigated the contribution of immune cells (macrophages, T-cells, neutrophils) to neuroinflammation, showing that they play a dual role in both initiating and perpetuating chronic pain, making them potential targets for immunomodulatory therapies [48]. Ji and colleagues in 2014 performed an extensive review examining how neuroinflammation drives the progression from acute to chronic pain. Their analysis revealed that persistent activation of glial cells particularly microglia and astrocytes induce dysfunctional synaptic remodeling, heightened neuronal excitability, and pain-related memory formation in both the spinal cord and brain. Their findings underscored the importance of identifying specific biomarkers and developing targeted therapies that modulate glial activity and inflammatory cascades [49].

In a 2022 investigation, Duan and colleagues elucidated the role of TNF-α-mediated necroptosis in neuropathic pain pathogenesis, demonstrating its involvement in neuroimmune interactions within the pain pathway. Their work provided mechanistic insights into how this programmed cell death process contributes to pain sensitization through immune cell-neuron crosstalk in the nervous system. They demonstrated that TNF-α not only functions as a pro-inflammatory cytokine but also directly initiates programmed necrotic cell death (necroptosis), worsening neuronal injury and perpetuating chronic pain. This research highlights the potential for new treatment strategies aimed at inhibiting TNF-α signaling or blocking necroptotic pathways [50]. Atta and his colleagues in 2023 performed a comprehensive review exploring the role of microglial polarization in nociplastic and inflammatory pain. The study revealed that pro-inflammatory mediators (IL-1β, TNF-α, and nitric oxide) participate in complex, bidirectional signaling networks rather than simple linear pathways. These dynamic neuroimmune interactions create positive feedback mechanisms that amplify nociceptive signaling. Specifically, the reciprocal communication between activated glial cells and neuronal pathways establishes a self-perpetuating cycle that maintains chronic pain states. These findings highlight the therapeutic potential of modulating microglial reactivity and

interrupting cytokine-mediated signaling cascades as innovative approaches for pain management [51].

In their 2024 study, Kaye and colleagues examined the efficacy of TNF-α and interleukin pathway modulators (including IL-1β and IL-6) for treating persistent and pathological pain conditions. Through comprehensive evaluation of both animal studies and human clinical trials, the research team established that suppressing inflammatory cytokines significantly reduces pain sensitization and disrupts central pain processing pathways. This work supports the clinical relevance of cytokine focused treatments for managing chronic pain syndromes with inflammatory components [52].

The NOD-like receptor family, pyrin domain containing 3 (NLRP3) inflammasome is a multiprotein complex that plays a pivotal role in the pathophysiology of neuroinflammatory pain. Following stimulation by extracellular ATP, reactive oxygen species, or bacterial endotoxins, the NLRP3 inflammasome complex undergoes oligomerization and recruits the adaptor protein Apoptosis-associated Speck-like protein containing a caspase activation and recruitment domain (ASC). This recruitment facilitates the proteolytic activation of caspase-1, initiating the inflammatory cascade. This in turn promotes the maturation and release of IL-1β and IL-18, cytokines that significantly enhance nociceptive signaling and glial activation. Inhibition of NLRP3 components has shown promise in reducing hyperalgesia and allodynia in rodent models, highlighting its potential as a drug target in chronic pain syndromes [53].

2.2 Comparative Analysis of Neuroinflammatory Pain Animal Models

Various animal models are utilized to replicate the multifaceted aspects of neuroinflammatory pain. The CFA model is widely used to study localized peripheral inflammation, eliciting robust immune responses and hyperalgesia. In contrast, spinal nerve ligation (SNL) and chronic constriction injury (CCI) are better suited

for investigating neuropathic and neuroinflammatory pain mechanisms. SNL induces pronounced mechanical allodynia by selectively injuring spinal nerve roots, while CCI mimics chronic nerve compression, leading to progressive neurodegeneration and persistent immune activation. For systemic and central neuroinflammation, lipopolysaccharide (LPS) and polyinosinic-polycytidylic acid are frequently utilized. These agents activate Toll-like receptors (TLRs), promoting cytokine release (e.g., TNF-α, IL-6) and microglial/astrocyte activation, thereby modeling neuroinflammatory pain with broader immunological involvement. These models are particularly valuable for investigating neuroimmune interactions and assessing the efficacy of anti-inflammatory treatments targeting central nervous system pain pathways [54]. Hyperalgesia and mechanical allodynia are hallmark features of neuropathic and neuroinflammatory pain conditions. Hyperalgesia involves an abnormally heightened pain response to stimuli that are normally painful, reflecting an increased sensitivity of the nervous system. In contrast, mechanical allodynia occurs when typically, non-painful stimuli such as light touch, gentle pressure, or brushing of the skin trigger pain. Both conditions result from maladaptive changes in pain processing, including peripheral and central sensitization, where neurons become excessively responsive to sensory input. These abnormal pain responses are key indicators of nerve dysfunction and play a critical role in chronic pain disorders [55].

2.3 Computational Approaches in Neuroinflammation Drug Discovery

The integration of molecular docking with ADME evaluation has revolutionized initial drug discovery processes. Through in silico modeling, researchers can predict the binding affinity of potential drug candidates to inflammatory targets like TNF-α, IL-1β, and NF-κB. Computational ADME modeling concurrently evaluates critical pharmacokinetic parameters, including gastrointestinal absorption, blood-brain barrier permeability, and hepatic metabolic resistance. This predictive capability facilitates structure-guided optimization of lead compounds,

particularly for neurotherapeutic development. By merging in silico screening with physicochemical profiling, researchers can systematically prioritize candidates with desirable CNS activity while reducing reliance on animal studies. Such integrative computational strategies markedly improve both the throughput and accuracy of identifying viable neuroinflammatory therapeutics.

2.4 Limitations of Current Treatments and Novel Approaches

Gupta & Bah in 2022 systematically evaluated the organ-specific toxicity of NSAIDs, encompassing gastrointestinal, cardiovascular, renal, and hepatic effects. Their analysis confirmed that while NSAIDs effectively alleviate pain through cyclooxygenase (COX) inhibition, prolonged use even at therapeutic doses carries significant risks, including upper GI ulceration, hypertension, myocardial infarction, and renal impairment [56]. In their 2015 study, Yeomans and colleagues systematically evaluated safety data from randomized controlled trials and meta analyses examining different NSAID classes. Their analysis revealed distinct risk profiles: COX-2 selective agents like celecoxib demonstrated reduced gastrointestinal toxicity, while traditional NSAIDs such as ibuprofen and naproxen showed increased cardiovascular adverse effects. These findings emphasized the need for individualized NSAID therapy, taking into account patient characteristics including age and pre-existing medical conditions [56]. Oxidative and nitrosative stress are well-recognized contributors to neuropathic and inflammatory pain. The physiological equilibrium between reactive oxygen species (ROS) and reactive nitrogen species (RNS) and their endogenous antioxidant counterparts is crucial for cellular homeostasis. Disruption of this balance leads to several pathological consequences: impaired mitochondrial activity, enhanced neuronal hyperexcitability, and oxidative modifications to cellular macromolecules including nucleic acids and structural proteins. Key oxidative mediators such as superoxide anions (O_2^-), hydrogen peroxide (H_2O_2), and peroxynitrite ($ONOO^-$) contribute to central sensitization through multiple mechanisms - principally via NMDA receptor potentiation and

post-translational protein nitration within spinal cord pathways. Furthermore, these reactive species activate microglia and astrocytes, stimulating the release of pro-inflammatory cytokines that establish and maintain chronic neuroinflammatory states.

In rodent studies, antioxidant therapies such as scavengers, enzyme mimetics, or NADPH oxidase (NOX) inhibitors have demonstrated significant effectiveness in reducing mechanical allodynia and thermal hyperalgesia [57, 58].

2.5 Benzothiazole Derivatives as Promising Therapeutics

Recent research has increasingly focused on heterocyclic compounds, particularly benzothiazole derivatives, due to their pharmacological versatility. Badgujar and his colleagues in 2024 highlighted the anti-inflammatory, antimicrobial, and anticancer properties of 2-aminobenzothiazole scaffolds, making them attractive candidates for drug development [20]. Azam in 2011 emphasized benzothiazole's ability to cross biological membranes, including the blood-brain barrier, which is crucial for targeting neuroinflammatory conditions [31].

In their 2020 study, Bhat and Belagali employed click chemistry techniques to develop novel hybrid compounds combining 2-mercaptobenzothiazole and triazole moieties. These synthetic derivatives exhibited significant anti-inflammatory and pain-relieving properties, showing efficacy similar to the standard drug ibuprofen while displaying a more favorable safety profile with reduced adverse effects [33]. In 2018 investigation, Tariq and his colleagues systematically refined benzothiazole derivatives through targeted molecular modifications. Their structure-activity relationship studies revealed that these chemical alterations significantly improved both pharmacokinetic properties and therapeutic efficacy. The researchers identified JNK pathway suppression as a key mechanism underlying the compounds enhanced anti-inflammatory effects, demonstrating improved biological availability compared to earlier analog [59]. In 2023 study, Yadav and colleagues investigated

fluorinated analogs of benzothiazole compounds, demonstrating that strategic fluorine substitution significantly enhances both lipid solubility and resistance to metabolic degradation. These pharmacological improvements were shown to increase the compounds efficacy in treating neuroinflammatory pain conditions, suggesting promising clinical applications [60]. A. A. Abbas and his colleagues in 2024 investigated thiodiazole-benzothiazole hybrids, revealing that these modifications improve drug-target interactions, leading to safer and more effective treatments [40]. Vedavathi and his colleagues in 2010 concluded that combining fluorine and thiodiazole in benzothiazole scaffolds holds significant promise for next-generation anti-inflammatory drugs [42].

Chapter 3

Material and Methods

3.1 Introduction

This chapter provides a comprehensive overview of the experimental design and methodologies employed to evaluate the neuroinflammatory and analgesic potential of fluorinated mercaptobenzothiazole derivatives in a well-established model of neuroinflammatory pain. Given the intricate nature of neuroinflammation characterized by a dynamic interplay of immune responses, neuronal signaling, and molecular mediators, the experimental approach was meticulously structured to ensure scientific rigor, reproducibility, and ethical compliance.

To simulate chronic inflammatory pain conditions reflective of human pathophysiology, CFA was administered to induce persistent peripheral inflammation. Male Balb/C mice, selected for their consistent physiological responses and genetic homogeneity, served as the biological model to reduce experimental variability and enhance translational value. A multimodal assessment strategy was adopted to capture various dimensions of pain and inflammation. Behavioral responses were quantified using validated tests such as the hot plate test (thermal hyperalgesia), von frey filaments (mechanical allodynia), and paw edema evaluation via digital

calipers. These *in vivo* observations were complemented by biochemical and histological analyses, including protein quantification, cytokine profiling through ELISA, and tissue morphology assessment via histopathological staining.

To further elucidate the pharmacodynamic profile of the test compound, silico techniques were employed. Molecular docking studies and ADME (Absorption, Distribution, Metabolism, and Excretion) profiling were conducted to explore potential molecular interactions with key inflammatory mediators and predict the compound's drug-likeness. All experimental procedures were performed in accordance with internationally accepted ethical standards and institutional guidelines.

The detailed methodologies presented in this chapter establish a robust framework for understanding the pharmacological evaluation of fluorinated mercaptobenzothiazole derivatives as potential therapeutic agents in the management of neuroinflammatory pain.

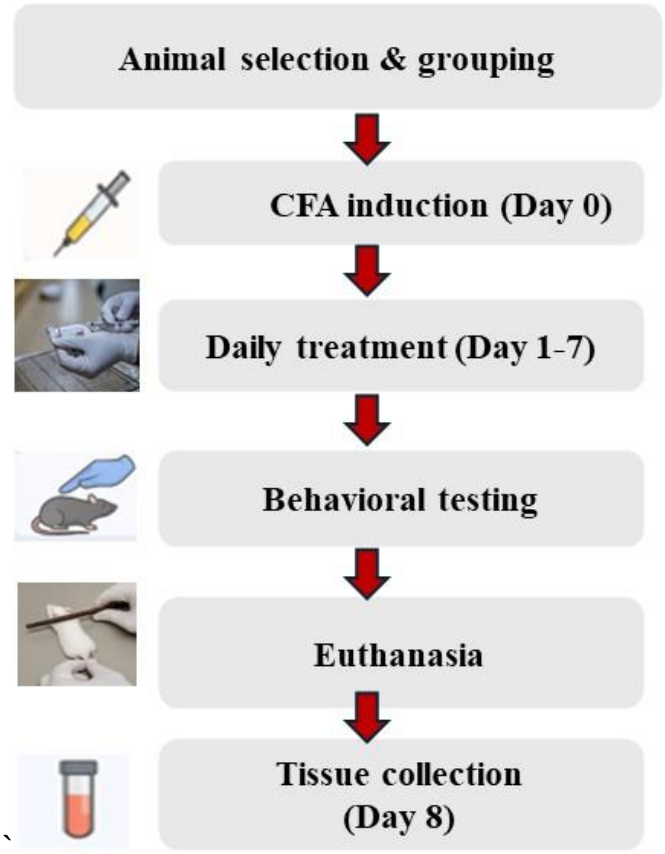

FIGURE 3.1: Experimental Workflow Diagram

The above diagram outlines the sequential steps followed during the *in vivo* study to evaluate the neuroinflammatory test compounds. The experiment began with animal selection and grouping, followed by the induction of inflammation using complete Freund's adjuvant (CFA) on Day 0.

From Days 1 to 7, animals received daily treatment with the respective compounds. Behavioral testing was conducted to assess pain-related responses. At the conclusion of the study, animals were humanely euthanized, and relevant tissues were collected for further biochemical and histological analysis.

3.2 Ethical Considerations

Every aspect of the study involving animals was carried out in full compliance with international and national ethical standards concerning the humane treatment and use of laboratory animals. The research protocol was thoroughly reviewed and approved by the Institutional Animal Ethics Committee (IAEC) of the Capital University of Science and Technology (CUST), Islamabad, (Approval No. REC/FoP/F2024/01) prior to commencement.

The study adhered to the guidelines issued by the U.S based Association for Assessment and Accreditation of Laboratory Animal Care International (AAALAC) for humane treatment and welfare of Balb/C mice used in this study ensuring that the research was conducted under legally and ethically approved conditions.

The principle of the 3Rs Replacement, Reduction, and Refinement was stringently followed throughout the research [61]. The concept of Replacement was addressed by using animals only where no valid non-animal alternative was available. Reduction was implemented by using the minimum number of animals necessary to achieve statistically valid results, thus avoiding unnecessary use of experimental subjects. Refinement was ensured by optimizing all procedures to minimize pain, stress, and discomfort to the animals. All personnel involved in animal handling and experimentation were well-trained and experienced in laboratory animal management and ethical research practices.

Regular monitoring was carried out twice daily throughout the study to assess the animals' general health, food and water intake, grooming behavior, posture, and overall physical condition. Any animal that showed signs of illness, extreme weight loss, abnormal behavior, or visible injury was examined and attended to appropriately under the supervision.

The aim was to guarantee that the animals were treated with the highest level of care and respect as living subjects in a scientific investigation.

3.3 Experimental Animals

This study was conducted using healthy, young adult male Balb C mice, which are widely recognized as an ideal model for pharmacological and neuroinflammatory research due to their well-documented genetic consistency, manageable size, and predictable behavioral responses. The total number of animals used in the study was forty-five (45), with each animal carefully selected to match the inclusion criteria, namely, a body weight ranging between 25 to 30 grams. These animals were neither genetically modified nor previously exposed to any form of pharmacological or behavioral testing, ensuring the biological integrity and experimental reliability of the model.

FIGURE 3.2: Measurement of mouse body weight using balance

As the above figure shows the animal's weighing was performed using a digital scale (SF-400C model) prior to dosing and behavioral testing to monitor any weight changes during the experimental protocol. Accurate body weight assessment was essential for dose calculation and evaluating the general health status of the animal throughout the study. (Photograph captured at the Faculty of Pharmacy, Capital University of Science and Technology).

3.4 Environmental Maintenance

All animals were housed in a controlled, pathogen-free environment within standard laboratory animal cages. The cages used were made of high-quality polycarbonate material, with transparent walls to allow clear observation of animal behavior and a secure stainless steel wire mesh lid for ventilation.

The bedding material used in the cages consisted of common bedding include wood shaving such as aspen, which is absorbent, non-toxic, and comfortable for the animals. Bedding was changed regularly typically every 24 hours, or earlier if soiled to maintain hygiene and prevent the build-up of ammonia and microbial contaminants. All cages and water bottles were thoroughly washed and sterilized before reuse to maintain aseptic conditions.

FIGURE 3.3: Laboratory housing of BALB/c mice under standard conditions

As shown in the above figure, BALB/c mice were housed in a standard polycarbonate cage containing wood chip bedding. The cage environment was maintained to support animal comfort, hygiene, and natural behavior during the experimental

period. These conditions were ensured in accordance with institutional animal care guidelines for the ethical handling of laboratory animals in preclinical research. (Photograph captured at the Faculty of Pharmacy, Capital University of Science and Technology, Islamabad).

Environmental conditions were maintained within an optimal range as per international laboratory animal care standards. Ambient temperature was regulated to remain consistently between 22 ± 2°C, providing a comfortable thermo neutral zone for mice. Relative humidity was carefully controlled between 50% and 60%, using humidifiers and dehumidifiers as needed, to protect against dehydration and respiratory issues that may arise from overly dry or moist air.

The animal holding room was subjected to a 12-hour light/dark cycle, with lights switched on, simulating a natural circadian rhythm. Artificial lighting was soft and evenly distributed to avoid light stress or disorientation in the animals. The room was well-ventilated ensuring a constant flow of fresh air, reduction in odor, and prevention of airborne pathogen accumulation.

Animals were provided with unrestricted access to a standard pellet diet and clean drinking water throughout the course of the study [62]. Drinking water was provided in sterilized glass bottles equipped with stainless steel sipper tubes, and bottles were replenished with clean, filtered water daily. Water sources were monitored for microbial contamination as per animal care protocols [63].

TABLE 3.1: Composition of animals' food

Food item	**5.0 kg**	**10.0 kg**	**20.0 kg**	**40.0 kg**
Wheat Flour	3.25 Kg	6.5 Kg	13 Kg	26 Kg
Chokar	750 g	1. 5 Kg	3.0 Kg	6.0 Kg
Fish	750 g	1. 5 Kg	3.0 Kg	6.0 Kg
Dry Skimmed Milk	200 g	400 g	800 g	1600 g
Vitamins/Minerals*	75 g	150 g	300 g	600 g

Noise levels in the facility were kept to a minimum to avoid auditory stress, which can negatively affect the behavior and hormonal balance of rodents. Handling of

animals during cage cleaning or data collection was performed gently and efficiently by trained personnel using proper techniques to avoid injury or stress. Animals were not subjected to any unnecessary handling, and any procedures involving physical interaction were performed with calmness and care [64].

FIGURE 3.4: Proper handling technique for experimental mice

This gentle handling method was used to minimize stress and ensure the animal's comfort during routine experimental procedures, in accordance with ethical animal care practices. (Photograph captured at the Faculty of Pharmacy, Capital University of Science and Technology).

3.5 Gender Determination in Rodents

The sex of mice was determined by measuring distance the anogenital (AGD) the space between the anal and genital openings. Males exhibit a significantly greater AGD than females, allowing for reliable and non-invasive sex differentiation.

3.6 Randomization and Animal Identification

To ensure unbiased group allocation, all animals were randomly assigned to experimental groups. For individual identification throughout the study period, a tail-marking system was implemented using combinations of short and long transverse lines. Randomization of the animals was done in order that there is no skewed data for each experimental group.

The animals were marked on tail for their proper identification before starting the experiment. The marking was as followed:

Animal # 1. One circle having small cross-sectional area was drawn across the tail.

Animal # 2. Two circles having small cross-sectional areas and separated from each other by little space were drawn across the tail.

Animal # 3. Three circles having small cross-sectional areas and separated from each other by little space were drawn across the tail.

Animal # 4. Four circles having small cross-sectional areas and separated from each other by little space were drawn across the tail.

Animal # 5. One circle having large cross-sectional area was drawn across the tail.

Animal # 6. Two circles, 1^{st} having large cross-sectional area and 2^{nd} having small area cross sectional and separated from each other by little space were drawn across the tail.

Animal # 7. Three circles, 1^{st} having large area cross sectional and 2^{nd} and 3^{rd} having small area cross sectional and separated from each other by little space were drawn across the tail.

Animal # 8. Four circles, 1^{st} having large area cross sectional and 2^{nd}, $3^{rd}$and 4^{th} having small area cross sectional and separated from each other by little space were drawn across the tail and so on for higher numbers.

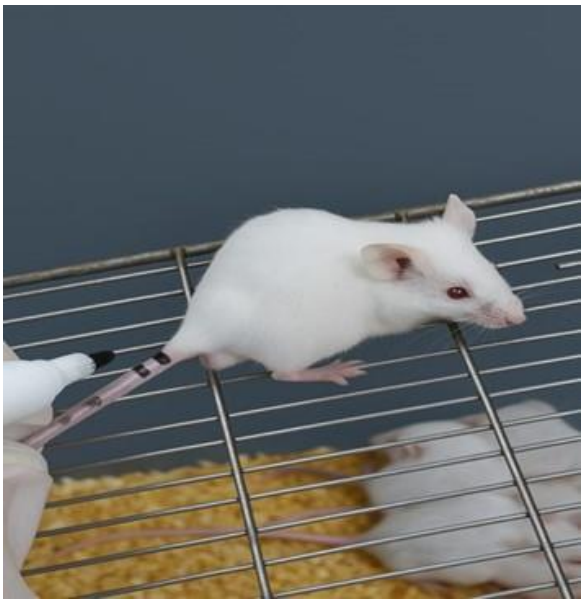

FIGURE 3.5: A tail-marking system was implemented using combinations of short and long transverse lines

This systematic approach allowed for clear and immediate identification of each subject while minimizing handling stress. The markings were applied using non-toxic, semi-permanent ink and were refreshed as needed to maintain visibility throughout the experimental timeline.

The method proved particularly advantageous as it was both non-invasive and easily scalable should additional animals be required for the study.

3.7 Grouping and Experimental Design

A well-structured experimental protocol was designed to evaluate the therapeutic efficacy of the fluoro-mercaptobenzothiazole derivative in animal model of inflammatory pain. The study was conducted over a seven-day period following the induction of inflammation and utilized a total of 45 healthy adult albino mice. These animals were randomly divided into five groups, with nine animals (n = 9) allocated to each group. The grouping was performed manually to ensure a balanced distribution of body weight and baseline activity among groups, thus minimizing inter-individual variability and bias.

TABLE 3.2: Summary of experimental animal groups with their respective treatments and objectives

Group No.	**Group Name**	**Treatment Details**	**Study Objective**
Group I	Vehicle Control	Received intraperitoneal (i.p.) injection of sterile vehicle only. No CFA was administered.	Establishes baseline physiological and behavioral responses in healthy animals.
Group II	Negative Control	Received CFA injection (intraplantar, right hind paw) without any therapeutic intervention.	Serves as an untreated control to evaluate CFA-induced inflammation and pain-like behavior.
Group III	Positive Control	Post-CFA induction, treated with diclofenac sodium (5 mg/kg, i.p., once daily).	Benchmarks anti-inflammatory and analgesic effects of a known NSAID.
Group IV	Low Dose Test Group	Post-CFA, administered FMBT at 5 mg/kg (i.p., once daily).	Evaluates the test compound's potential to reduce inflammation and pain at a low dose.
Group V	High Dose Test Group	Post-CFA, administered FMBT at 10 mg/kg (i.p., once daily).	Assesses dose-dependent neuroinflammatory and analgesic effects of the test compound.

3.8 Induction of Inflammation

As shown in the figure, following intraplanar administration of CFA, the paw displays pronounced swelling and redness, indicative of peripheral inflammation. This model replicates neuroinflammatory pain conditions and is widely used to evaluate the neuroinflammatory potential of test compounds, including fluorinated mercaptobenzothiazole derivatives used in the current study. (Photograph captured at the Faculty of Pharmacy, Capital University of Science and Technology).

CFA is a potent immunological agent widely used in research to enhance the body's immune response to antigens. Developed by Jules Freund in the 1940s,

FIGURE 3.6: CFA-induced swelling and redness in the right hind paw of a Balb/C mouse, representing localized inflammatory response

CFA is a water-in-oil emulsion comprising non-metabolizable oils like paraffin oil and mannide monooleate, combined with heat-killed *Mycobacterium tuberculosis* bacteria [65].

To replicate persistent inflammatory pain condition, CFA was used to induce localized inflammation in the right hind paw of the mice. A single dose of CFA (20 μL) was administered intraplantarly under mild restraint, without the use of anesthesia, to model a inflammatory state that mimics key features of human pain [66]. Following induction of inflammation, animals were subjected to respective treatment protocols based on their group allocations. All animals were monitored throughout the 7-day experimental period for behavioral changes, signs of inflammation, and any adverse reactions to the treatments. Behavioral assessments and pain threshold analyses were conducted at defined intervals to compare the therapeutic efficacy across the different groups. This experimental design enabled a robust and controlled evaluation of the neuroinflammatory potential of the fluoro-mercaptobenzothiazole compound in comparison with both vehicle treated and standard drug-treated controls.

To establish a reliable and reproducible model of neuroinflammatory pain, CFA was employed to induce localized inflammation in the right hind paw of experimental mice [67]. CFA is a well-established immunological agent extensively used in preclinical research for its ability to simulate inflammatory conditions resembling human arthritic and neuropathic pain syndromes [68].

On the initial day of the study (Day 0), all experimental groups scheduled for complete Freund's adjuvant administration (including Negative Control, Standard Drug, MBT 5 mg/kg, and MBT 10 mg/kg received inflammatory induction. The animals were manually restrained without anesthetic administration to prevent stress-related physiological changes.

Using a precision micro syringe equipped with a thin-gauge needle, 20 μL of CFA solution was administered via intraplantar injection into the central area of the right posterior limb. This specific injection location was selected to produce a focused inflammatory reaction while reducing both tissue trauma and potential systemic dissemination of the adjuvant.

The CFA employed in this investigation was formulated as an oil-based suspension incorporating inactivated *Mycobacterium tuberculosis* cells dispersed in a mineral oil vehicle. This preparation induces a characteristic cell-mediated immune response that results in pronounced paw swelling, heightened pain sensitivity in affected tissues, and elevated levels of pro-inflammatory signaling molecules such as interleukins, eicosanoids, and sensory neuron-derived peptides. These physiological changes accurately reproduce the key features of chronic inflammatory pain conditions.

Table 3.3: Drugs and chemicals used

Sr.	**Chemical/Substance**	**Source**
1	Complete freund's adjuvant	Unknown
2	Diclofenac sodium	Uknown
3	Mercaptobenzothiazole (derivative)	Synthesized in lab / precursor from Sigma-Aldrich
4	Dimethyl sulfoxide (DMSO)	Sigma-Aldrich
5	Chloroacetyl chloride	Sigma-Aldrich
6	Dichloromethane	Sigma-Aldrich
7	Triethylamine	Sigma-Aldrich
8	Benzylamine	Sigma-Aldrich
9	Acetonitrile	Sigma-Aldrich
10	Potassium carbonate	Sigma-Aldrich
11	Potassium iodide	Sigma-Aldrich
12	Sodium sulphate anhydrous	Sigma-Aldrich

3.9 Treatment Groups and Dosing

3.9.1 Drug Administration Protocol

The drug administration protocol in this study was carefully designed to follow a structured and scientifically sound sequence of steps that allowed accurate observation of therapeutic effects in the CFA-induced inflammatory pain model. The protocol was initiated with baseline behavioral assessments at 0 hours (pre-CFA induction).

These baseline measurements were critical in establishing the normal physiological and nociceptive response profiles of all animals prior to the onset of inflammation.

Following the recording of baseline data, CFA was administered via a single intraplantar injection into the right hind paw of each animal (except those in the vehicle control group), effectively inducing localized inflammation that mimics neuroinflammatory conditions.

Treatment administration was commenced after the induction of inflammation and continued once daily for seven consecutive days. This post-induction treatment design allowed for the assessment of therapeutic efficacy under established inflammatory conditions.

FIGURE 3.7: Intraperitoneal administration of test compound in a Balb/C mouse

As demonstrated in the figure, Intraperitoneal injection was performed using sterile technique to deliver the test compound into the peritoneal cavity for systemic absorption.

This route ensures rapid and consistent bioavailability, making it suitable for evaluating the *in vivo* pharmacological effects of fluorinated mercaptobenzothiazole derivatives in the CFA-induced Neuroinflammatory pain model. (Photograph captured at the Faculty of Pharmacy, Capital University of Science and Technology, Islamabad).

3.9.2 Dose Preparation

The test compound, fluoro-mercaptobenzothiazole, was prepared in two distinct doses 5 mg/kg and 10 mg/kg to evaluate its dose-dependent effects.

The drug was freshly prepared each day prior to administration to preserve its pharmacological potency and stability.

3.9.2.1 Drug Solubility

Given the limited aqueous solubility of the test compound, initial dissolution attempts in normal saline using vortexing proved ineffective.

To enhance solubility, a co-solvent strategy was adopted, wherein 40 μL of dimethyl sulfoxide (DMSO) was introduced to the compound in an Eppendorf tube, followed by vigorous vortexing to achieve complete dissolution.

3.9.2.2 Dose Calculation

The dosage volume for each mouse was calculated according to its individual body weight using the standard dose formula:

Required dose (mg/kg) $\times$ Body weight (kg) = Dose per mouse (mg)

To prepare the drug solutions for intraperitoneal injection, the required concentrations were formulated using a mixture of DMSO and normal saline.

3.9.2.3 Dose Preparation of Mercaptobenzothiazole Derivative

For the 5 mg/kg dosage, 0.5 mg/kg of the compound was initially dissolved in 40 μL of DMSO within an Eppendorf tube, after which 950 μL of normal saline was added. The mixture was then thoroughly vortexed to ensure complete solubilization.

3.9.2.4 Dose Preparation of Mercaptobenzothiazole Derivative

In the case of the 10 mg/kg dosage, 1 mg of the compound was combined with 40 μL of DMSO, followed by the addition of 950 μL of normal saline. The solution was vortexed again until it appeared uniformly dissolved and free of particulate matter.

The appropriate volume was then measured based on each animal's weight and administered intraperitoneally using sterile 1 mL syringes with insulin needles, under strict aseptic conditions. Each animal received its respective treatment once daily for seven days.

3.10 Behavioral Assessment

To comprehensively evaluate the progression of neuroinflammatory pain and the therapeutic efficacy of the test compound, a series of behavioral assessments were conducted throughout the experimental period. The behavioral evaluation encompassed measurements of thermal nociception, mechanical allodynia, and inflammatory swelling. These assessments were carried out on a daily basis for seven consecutive days, beginning from Day 0 (baseline) prior to the induction of inflammation and continuing through Day 7. This allowed a consistent and comparative analysis of pain-related behaviors in response to CFA administration and subsequent treatment.

All animals were acclimatized to the testing environment prior to assessment each day to reduce stress-induced variability. Each behavioral parameter was measured using a consistent schedule and standardized protocol for all groups.

3.10.1 Hot Plate Test

The hot plate test was employed to evaluate central thermal nociceptive responses, which are commonly heightened in neuroinflammatory pain models. This test is widely recognized for assessing thermal hyperalgesia, especially in response to centrally mediated noxious stimuli.

In the current study, the hot plate apparatus was calibrated to maintain a consistent surface temperature of 55 ± 0.5°C. The platform was constructed of a metallic surface enclosed within transparent acrylic walls, ensuring both safety and visibility during the test. Each mouse was gently placed on the heated surface, and the response latency (in seconds) was measured as the time interval between placement and the exhibition of any nociceptive response.

Typical pain related behaviors observed included paw licking, flicking, lifting, or sudden jumping. A manual start-stop trigger was attached. The stopwatch was started at the moment the mouse was placed on the plate and was stopped immediately upon the first sign of nociceptive behavior. This method ensured precise timing of response without relying on automated tracking. To ensure ethical compliance and avoid tissue damage, a strict cut-off latency of 30 seconds was observed. If no response occurred within this time frame, the mouse was immediately removed from the plate to prevent thermal injury.

This test was conducted once daily for each mouse. Baseline readings (Day 0) were recorded prior to CFA injection, followed by assessments on each of the subsequent six days (Days 1–7). This design facilitated accurate tracking of thermal pain progression and allowed evaluation of treatment efficacy over time [69].

As shown in the figure, the hot plate test was used to evaluate central thermal nociception. Mice were placed individually on a heated surface maintained at

52 ± 0.5 °C, and the latency to exhibit pain-related behaviors (such as paw licking or jumping) was recorded.

A decrease in latency indicated hyperalgesia, while increased latency post-treatment reflected analgesic efficacy. (Photograph captured at the Faculty of Pharmacy, Capital University of Science and Technology).

FIGURE 3.8: Hot plate apparatus used for evaluating thermal hyperalgesia in rodents

The hot plate test was used to evaluate central thermal nociception. Mice were placed individually on a heated surface maintained at 52 ± 0.5 °C, and the latency to exhibit pain-related behaviors (such as paw licking or jumping) was recorded. A decrease in latency indicated hyperalgesia, while increased latency post-treatment reflected analgesic efficacy. (Photograph captured at the Faculty of Pharmacy, Capital University of Science and Technology).

3.10.2 Von Frey Filament Test

To assess mechanical hypersensitivity associated with neuroinflammation, the von frey filament technique was utilized. This method measures the animal's response to innocuous mechanical stimuli and is a reliable indicator of mechanical allodynia, a key feature of chronic inflammatory pain. Mice were individually placed in transparent plexiglass chambers positioned over an elevated wire mesh platform that permitted access to the plantar surface of their hind paws. The animals were allowed to acclimate to the testing environment for a minimum of 20–30 minutes before each assessment, ensuring they were calm and stationary before stimulus application [70].

A series of calibrated von frey filaments were applied perpendicularly to the plantar surface of the CFA-injected hind paw. The force was applied just enough to cause a gentle bend in the filament, ensuring a standardized pressure stimulus.

Each filament was applied for a duration of approximately 1–2 seconds, and a positive response was considered if the animal demonstrated behaviors such as sudden paw withdrawal, flinching, licking, or shaking of the stimulated paw. [19, 71].

FIGURE 3.9: Von frey filament test to assess mechanical allodynia

Before testing, mice were placed individually under transparent plastic beakers on a mesh platform and allowed to acclimate for 15–30 minutes to minimize stress-induced behavioral variability. This acclimatization step was essential for obtaining reliable baseline paw withdrawal thresholds during the von frey filament test, which was used to assess mechanical allodynia associated with CFA-induced inflammatory pain. (Photograph captured at the Faculty of Pharmacy, Capital University of Science and Technology, Islamabad)

FIGURE 3.10: Complete set of calibrated von frey filaments used for mechanical allodynia testing

As given in the above figure, A set of standardized von frey monofilament used to assess mechanical allodynia in mice. Each filament was applied perpendicularly to the plantar surface of the hind paw until it bent slightly, and the paw withdrawal response was recorded. This method provided a quantitative measure of tactile sensitivity in CFA-induced inflammatory pain models. (Photograph captured at the Faculty of Pharmacy, Capital University of Science and Technology, Islamabad).

FIGURE 3.11: Von frey filament used for mechanical sensitivity testing in animal models

To evaluate mechanical hypersensitivity in Balb/C mice, a standardized von frey filament used, delivering a consistent force application. The filament was precisely administered to the ventral aspect of the posterior limb, with observed paw withdrawal responses serving as quantitative indicators of tactile allodynia.

This particular force threshold was chosen due to its established sensitivity in detecting CFA-mediated inflammatory hyperalgesia in animal models. (Photograph captured at the Faculty of Pharmacy, Capital University of Science and Technology).

3.10.3 Paw Edema Measurement

Paw edema is commonly assessed by measuring the thickness or diameter of the affected paw using a micrometer or caliper. This method provides a quick, non-invasive, and reproducible way to evaluate inflammation and the efficacy of anti-inflammatory agents in animal models.

3.10.3.1 Method Description

A precision micrometer or digital caliper is used to measure the mediolateral thickness of the hind paw at the site of edema, typically at fixed time intervals following the induction of inflammation. The change in paw thickness is calculated by comparing the baseline (pre-injection) measurement from the post-treatment value [72].

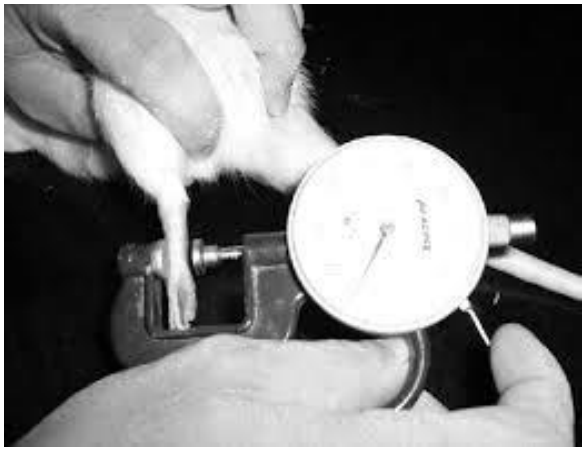

FIGURE 3.12: Measurement of hind paw edema thickness of a mice by micrometer [5]

As shown in figure above, the paw thickness was measured using a digital micrometer to evaluate the degree of inflammation following CFA administration. This method provides a quantitative assessment of peripheral edema, which serves as an indirect indicator of inflammatory severity. Consistent measurement at defined time points enabled comparison of neuroinflammatory effects of test compound.

3.11 Acute Toxicity and Ethical Termination Procedures

To evaluate the immediate safety profile of the test compound prior to its therapeutic application, an acute toxicity study was conducted following the standard protocols for *in vivo* toxicity testing. This preliminary study was designed to assess any potential acute adverse effects of the fluoro-mercaptobenzothiazole compound at a high dose in mice, ensuring that the selected treatment doses for the main experiment fall within a safe biological range.

For this study, eight healthy adult Balb/C mice were selected and housed under standard laboratory conditions. The environmental conditions were maintained at a temperature of 22 $\pm$ 2°C, relative humidity of 50–60%, with a 12-hour light/dark cycle. The mice were provided with a standard laboratory diet and water ad libitum and were allowed to acclimatize to the animal house environment for at least one week prior to the experiment.

Each mouse received a single intraperitoneal (i.p.) dose of 100 mg/kg body weight of the test compound. The compound was prepared freshly on the day of administration. For the dose preparation, 1 mL of vehicle solution was used, consisting of 40 μL DMSO, 950 μL normal saline, to ensure uniform solubility and appropriate dispersion of the compound. Following administration, the animals were closely observed individually over a period of 24 hours.

The mice were monitored for any signs of acute toxicity, changes in behavior, physical appearance, feeding patterns, or abnormal motor activity. Parameters

such as general activity, posture, response to external stimuli, grooming behavior, and movement patterns were carefully noted.

This study was conducted to determine the safety margin of the compound and to guide the selection of appropriate lower doses (5 mg/kg or 10 mg/kg) for subsequent efficacy testing in the neuroinflammatory pain model (Idris et al., 2019).

FIGURE 3.13: Upright restraint technique used for intraperitoneal injection in mice

The upright manual restraint method was employed to immobilize the mouse safely during intraperitoneal administration of test compounds. Proper handling minimized stress and ensured accurate delivery of the solution into the lower right quadrant of the abdomen, avoiding internal organs. This technique was critical for maintaining consistency and animal welfare throughout the experimental protocol. (Photograph captured at the Faculty of Pharmacy, Capital University of Science and Technology).

3.12 Euthanasia and Tissue Collection

At the end of the experimental period, all animals were humanely euthanized for the purpose of tissue collection, which was necessary for further biochemical and histological analysis. The method used for euthanasia was cervical dislocation, a widely accepted physical method for sacrificing small laboratory animals. This

method was chosen because of its rapid action and effectiveness in causing immediate death without the use of chemicals that may interfere with subsequent tissue assays [73].

3.13 Cervical Dislocation Method

Cervical dislocation was carried out by firmly holding the mouse at the base of the skull using the thumb and forefinger of one hand, while the base of the tail or the hind limbs were gently but securely gripped with the other hand.

A quick and precise upward force was then applied to dislocate the cervical vertebrae from the skull, thereby severing the spinal cord and leading to immediate death. Care was taken to ensure that the technique was performed swiftly and without hesitation to minimize any potential suffering.

FIGURE 3.14: Cervical dislocation performed for humane euthanasia of the experimental mouse

As shown in above figure, the cervical dislocation was carried out as a method of euthanasia in accordance with institutional animal care guidelines and ethical approval protocols. This technique causes rapid loss of consciousness by dislocating the cervical vertebrae, minimizing pain and distress. (Photograph captured at the Faculty of Pharmacy, Capital University of Science and Technology).

Following the dislocation, the absence of vital signs such as heartbeat and respiratory movements was carefully observed to confirm death before proceeding to dissection. This method complies with the recommendations provided by various ethical and animal welfare organizations for the euthanasia of small rodents in biomedical research [74].

3.13.1 Tissue Collection Procedure

After confirmation of death, each animal was placed on a sterile dissection tray in the dorsal recumbent position. Dissection was carried out immediately to prevent tissue degradation. Using sterile surgical scissors and forceps, the skin and underlying muscle were carefully incised to expose the areas of interest for tissue collection.

3.13.2 Paw Tissue Collection

For the collection of inflamed paw tissue, the skin over the hind paw (previously injected with CFA, in the case of disease models) was gently removed to expose the soft tissue and muscle layers. A precise excision of the plantar surface of the paw was performed, ensuring that the area around the site of inflammation was included. The excised tissue was rinsed briefly in cold phosphate-buffered saline (PBS). The tissue samples were fixed in 10% formalin for histological processing.

3.13.3 Spinal Cord Extraction

Following paw tissue collection, spinal cord extraction was performed through a commonly used hydraulic extrusion method. The spinal column was first exposed by making a midline incision along the dorsal surface, followed by the removal of skin and muscle to reveal the vertebral column. The vertebral column was carefully severed at both the cervical and lumbar regions using sterile scissors. The entire spinal column was then isolated and placed in a petri dish.

To extrude the spinal cord, a 10 mL syringe filled with ice-cold PBS was fitted with a blunt needle or plastic tubing and inserted into the vertebral canal from the caudal (lumbar) end. Gentle pressure was applied to inject PBS through the canal, which caused the spinal cord to be expelled from the cranial end. The extruded spinal cord was then collected carefully using forceps, rinsed in cold PBS, and immediately transferred to appropriate containers. As with paw tissues, spinal cord samples were stored frozen for biochemical analysis [75].

All tissue samples were handled under sterile conditions to avoid contamination and preserve the integrity of the biological material.

The tools used during dissection were sterilized before and between each dissection to maintain consistency and reliability across all collected samples.

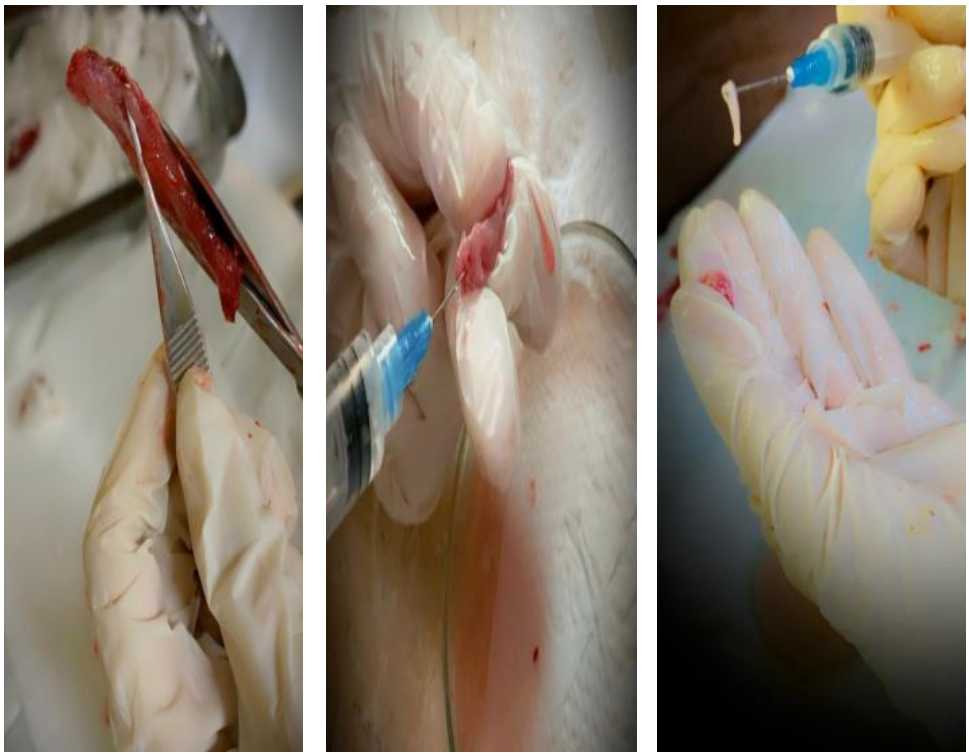

FIGURE 3.15: Spinal cord extrusion illustration. Schematic illustration of the spinal cord extrusion technique employed in this study

The spinal column was exposed via a midline dorsal incision with subsequent removal of overlying skin and muscle to reveal the vertebrae. The vertebral column was carefully severed at cervical and lumbar levels using sterile scissors and isolated. For spinal cord extrusion, a 10 mL syringe filled with ice-cold PBS and fitted with

a blunt needle or plastic tubing was inserted into the vertebral canal from the caudal (lumbar) end. Gentle pressure applied to the syringe expelled the spinal cord from the cranial end.

The extruded spinal cord was collected with forceps, rinsed in cold PBS, and stored frozen for further biochemical analysis. This hydraulic extrusion method provides a reliable and minimally traumatic approach for spinal cord extraction in experimental studies. (Photograph captured at the Faculty of Pharmacy, Capital University of Science and Technology).

3.14 Biochemical and Histological Analysis

3.14.1 Bicinchoninic Acid Assay

The Bicinchoninic Acid (BCA) assay was employed to quantify the total protein content in the spinal code. Tissue homogenization was performed using RIPA buffer at a ratio of 1 mL per 100 mg of sample. The homogenates were centrifuged at room temperature for 30 minutes at 8500 rpm to separate the supernatant, which was carefully collected for analysis.

For the assay, 10 μL of each sample was pipetted into a 96-well microplate. A series of standard protein dilutions was prepared at concentrations of 50 μg, 25 μg, 12.5 μg, and further serial dilutions down to 0 μg to construct a standard curve. Each well received a final volume of 10 μL.

The working reagent was freshly prepared by combining Reagent A and Reagent B in a 50:1 ratio (i.e., 50 parts Reagent A with 1 part Reagent B). This reagent was added to all wells containing either standards or test samples. The plate was then incubated at 37°C for 30 minutes.

Post incubation, absorbance was measured at 562 nm using a microplate reader. The protein concentrations in the test samples were calculated by comparing their absorbance values against the standard curve derived from the known concentrations.

3.14.2 Effect of MBT Derivative on Pro-inflammatory Cytokine Expression in Mice using Enzyme-linked Immunosorbent Assay

The levels of IL-1β and TNF-α were quantified through a sandwich ELISA approach employing, ELISA kit Ref No PRS-2050Mo, Lot No 202312, in strict adherence to the manufacturer's protocol. The assay utilized microtiter plates pre-coated with capture antibodies specific to mouse IL-1β or TNF-α. For calibration purposes, a standard curve was established by performing serial dilutions, initiating with 100 μL of the highest concentration standard in the initial wells, followed by successive dilutions with standard diluent in the remaining wells.

The test samples underwent a five-fold dilution by mixing 10 μL of each sample with 40 μL of diluent solution, after which 50 μL of the diluted mixture was carefully pipetted into the assigned wells.

Precautions were observed to prevent any contact with the well surfaces. Blank control wells contained neither sample nor conjugate. Following sample addition, the plates were securely covered and maintained at 37°C for a 30-minute incubation period.

Following incubation, the microplate wells underwent five washing cycles using wash buffer (prepared through 20-30× dilution of the stock solution with distilled water) to eliminate unbound components.

Subsequently, 50 μL of horseradish peroxidase (HRP) labeled detection antibody was dispensed into all wells excluding the blank controls, followed by a secondary 30-minute incubation period at 37°C. The plates were then subjected to an additional washing procedure.

For the color development step, 50 μL of both Chromogen Solution A and B were simultaneously introduced into each well, followed by a 15-minute dark incubation at 37°C.

The chromogenic reaction was terminated by the addition of 50 μL Stop Solution, which produced a distinct color transition from blue to yellow.

Absorbance was measured at 450 nm using a microplate reader within 15 minutes of adding the stop solution. The concentrations of IL-1β and TNF-α in the samples were calculated by comparing the optical density (OD) values to the standard curve derived from known concentrations.

FIGURE 3.16: Microplate reader used for ELISA analysis

The figure depicts the microplate reader used to measure absorbance at 450 nm for quantitative analysis in ELISA assays. This wavelength is optimal for detecting the colorimetric changes produced and enable precise determination of cytokine and biomarker concentrations in the samples analysed during this study.

3.14.3 Effect of MBT Derivative on Neuronal Survival using Hematoxylin and Eosin Staining

Tissue morphology and pathological changes were evaluated using the standard Hematoxylin and Eosin (H&E) staining method. Samples were first fixed in 10% neutral-buffered formalin for 24-48 hours at room temperature to maintain tissue structure. Following fixation, tissues were dehydrated through an ethanol gradient (70%, 80%, 95%, and 100%), then cleared in xylene. Automated processing

embedded the tissues in paraffin wax. The paraffin blocks were sectioned at 4-5 μm thickness, and slices were placed on glass slides. Slides were dried overnight at 37°C or for 1 hour at 60°C to ensure proper adhesion.

For the staining procedure, slides were dewaxed in xylene (two 5-minute immersions) and rehydrated through decreasing alcohol concentrations (100%, 95%, 70%). After a brief distilled water rinse, nuclei were stained with Harris hematoxylin for 5-7 minutes, followed by tap water rinsing. When necessary, nuclear differentiation was performed using 1% acid alcohol (1% HCl in 70% ethanol) for several seconds. Slides were then blued in 0.2% ammonia water or alkaline tap water for 1 minute.

Cytoplasmic staining was achieved with 1% eosin Y for 30-60 seconds, followed by distilled water rinsing. Slides were dehydrated through increasing alcohol concentrations (three 3-minute changes) and cleared in xylene. Coverslips were applied using xylene-based mounting medium. After drying, slides were examined under a bright-field microscope at 10× and 40× magnification to assess cellular morphology, tissue organization, and pathological changes. Images were recorded for further analysis.

3.15 In Silico Molecular Docking and ADME Analysis

3.15.1 Molecular Docking

Molecular docking represents a computational approach that forecasts the optimal spatial arrangement and binding strength between interacting molecules, most commonly a small molecule (ligand) and its biological target (receptor). This methodology serves as a fundamental tool in modern bioinformatics and pharmaceutical research, providing valuable insights into intermolecular recognition patterns and facilitating rational drug design strategies [76].

The process involves simulating the interaction between a ligand and its target protein to identify the most stable binding conformation. This simulation considers

various factors such as shape complementarity, hydrogen bonding, and hydrophobic interactions. Scoring functions are employed to estimate the binding affinity, providing insights into the strength and stability of the interaction.

Molecular docking has recently extended its applications from drug discovery to food science research. This computational approach now serves as an important method for investigating the binding relationships between nutritional constituents and biomolecular targets, supporting progress in dietary research and food quality assessment. Specifically, it helps elucidate the mechanisms by which food-derived bioactive molecules engage with human enzymes and cellular receptors, thereby affecting physiological responses.

The development of various molecular docking software, such as, AutoDock, has facilitated these studies by providing platforms to perform docking simulations efficiently. These tools allow researchers to model complex molecular interactions, predict binding modes, and assess the potential efficacy of compounds *in silico* before proceeding to experimental validation [77].

Overall, molecular docking serves as a bridge between computational predictions and experimental research, offering a cost-effective and time-saving approach to studying molecular interactions in both drug development and food science applications [78].

Virtual screening of chemical libraries has become an integral part of contemporary drug discovery processes. When a well-resolved structure of the target protein is available, molecular docking serves as an effective approach to distinguish potential binders from non-binders within extensive compound databases. This significantly reduces the number of candidates requiring experimental validation. The visual analysis of predicted binding orientations (docking poses) plays a pivotal role in optimizing lead compounds by enhancing binding affinity, minimizing adverse effects, and lowering the likelihood of resistance due to target mutations. In recent years, the PyMOL molecular graphics system has advanced from a robust 3D molecular visualization tool into a versatile platform that supports various applications, taking full advantage of its powerful rendering and analysis

capabilities [79]. Molecular docking studies were performed to investigate the potential interaction of the test compound with key pro-inflammatory protein targets involved in neuroinflammatory pain, including, IL-1 β, Tumor Necrosis Factor-alpha (TNF-α), and Nuclear Factor kappa B (NF-κB). These proteins were selected based on their established roles in inflammation and pain signaling pathways. The 3D structures of the target proteins were retrieved from the Protein Data Bank (PDB) in .pdb format. Prior to docking, proteins were prepared using AutoDock Tools (ADT), which involved the removal of water molecules, addition of polar hydrogens, and assignment of Kollman charges. Gasteiger charges were applied to the ligands.

The chemical structure of the test compound was initially sketched in ChemDraw before undergoing three-dimensional structural conversion via Open Babel software [80]. To optimize molecular stability, energy minimization was performed to obtain the lowest-energy conformation. The ligand structure was subsequently prepared in .pdbqt format, with defined torsional and rotatable bonds to ensure proper flexibility during docking. Using AutoDock software, molecular docking simulations were conducted. A grid box was constructed to encompass the active site residues of each target protein, enabling precise spatial mapping of ligand-receptor interactions within the binding pocket [81].

The docking simulations generated multiple potential binding conformations, from which the pose exhibiting the most favorable binding energy (indicating strongest affinity) was chosen for subsequent evaluation. Detailed examination was conducted on docking parameters including binding free energy (expressed in kcal/mol), hydrogen bonding patterns, van der Waals forces, π-π interactions, and hydrophobic contacts. Visualization and analysis of docking results were accomplished using PyMOL for three-dimensional structural representation and discovery studio visualizer for two-dimensional interaction mapping, facilitating the determination of key amino acid residues participating in ligand-receptor binding.

The molecular docking analyses enabled prediction of the test compound's spatial arrangement in the binding pockets of IL-1β, TNF-α, and NF-κB, offering valuable information about its possible neuroprotective effects. All computational

experiments were performed according to established docking methodologies to guarantee reliable and precise results [82].

3.15.2 In Silico Studies

In silico pharmacological studies serve as an essential component during the initial stages of drug development, providing crucial preliminary data prior to advancing to *in vivo* experimentation. These laboratory-based investigations establish the necessary scientific basis for evaluating drug candidates before progressing to animal studies [83].

In silico pharmacological research aims to examine drug-target interactions at molecular and cellular scales to assess therapeutic potential and safety profiles. The workflow commences with *target* discovery, involving investigation of disease pathways to identify modifiable biological targets such as specific proteins or receptors. Following target selection, high-throughput screening of compound libraries is conducted *in vitro* to identify initial active compounds ("hits") demonstrating target engagement or inhibitory effects. Subsequent *in silico* validation studies evaluate these hits for biological activity, target specificity, and potency using more sophisticated cellular models, including various cultured cell systems.

During this phase, computational approaches including molecular docking simulations are frequently employed in conjunction with experimental methods to model and forecast compound-target interactions. These *in silico* analyses yield valuable information regarding binding energetics and molecular conformations, though empirical validation using *in vitro* experiments remains crucial.

Following the selection of optimal candidate compounds, researchers progress to lead refinement a systematic process of structural modification aimed at enhancing pharmacological efficacy, minimizing adverse effects, and optimizing pharmacokinetic characteristics. All synthesized analogs are subjected to comprehensive *in vitro* assessment to determine key properties including target specificity, aqueous solubility, cellular toxicity, metabolic resistance, and binding potency.

Another major aspect of *in vitro* studies is safety pharmacology and early toxicity assessment, which is crucial to eliminate harmful compounds before they are tested in animals. Tools like ProTox-II or other computational and experimental toxicology platforms allow for high-throughput evaluation of toxicological risks, such as hepatotoxicity, cardiotoxicity, or genotoxicity. By identifying adverse effects early, researchers significantly reduce the number of compounds progressing to animal testing, thus saving time, resources, and minimizing ethical concerns related to animal use.

In summary, *in vitro* pharmacology is not just a preliminary step but a robust and essential screening system that filters out ineffective or harmful candidates, ensuring only the safest and most promising compounds move forward to *in vivo* studies. It provides a strong scientific rationale, based on detailed mechanistic understanding and safety profiling, which improves the success rate of later-stage drug development. This entire process enhances efficiency, cost-effectiveness, and ethical standards of drug discovery [84].

Chapter 4

Results

This chapter presents a detailed account of the experimental findings obtained during the evaluation of the pharmacological effects of a mercaptobenzothiazole-based compound in a preclinical model of neuroinflammatory pain. The results encompass multiple domains of investigation, including behavioral, biochemical, histological, *in silico* and toxicological assessments. Each of these components was carefully designed to explore different aspects of the compound's efficacy and safety profile.

Behavioral studies were conducted to assess changes in nociceptive and inflammatory responses over the course of treatment, while biochemical analyses provided molecular-level insights into cytokine modulation. Histopathological examination using Hematoxylin and Eosin (H&E) staining allowed microscopic evaluation of tissue integrity and inflammation. Additionally, acute toxicity testing was carried out in accordance with standard protocols to determine the compound's tolerability and potential adverse effects. The data obtained from these experiments are presented in the following sections, along with a comparative interpretation based on existing literature and mechanistic relevance. This integrated approach not only helps to validate the pharmacological potential of the test compound but also contributes to a broader understanding of its possible therapeutic application in neuro-inflammation.

4.1 Behavioral Assessments of Pain

4.1.1 Effects of MBT Derivative on CFA-induced Thermal Hyperalgesia in Mice

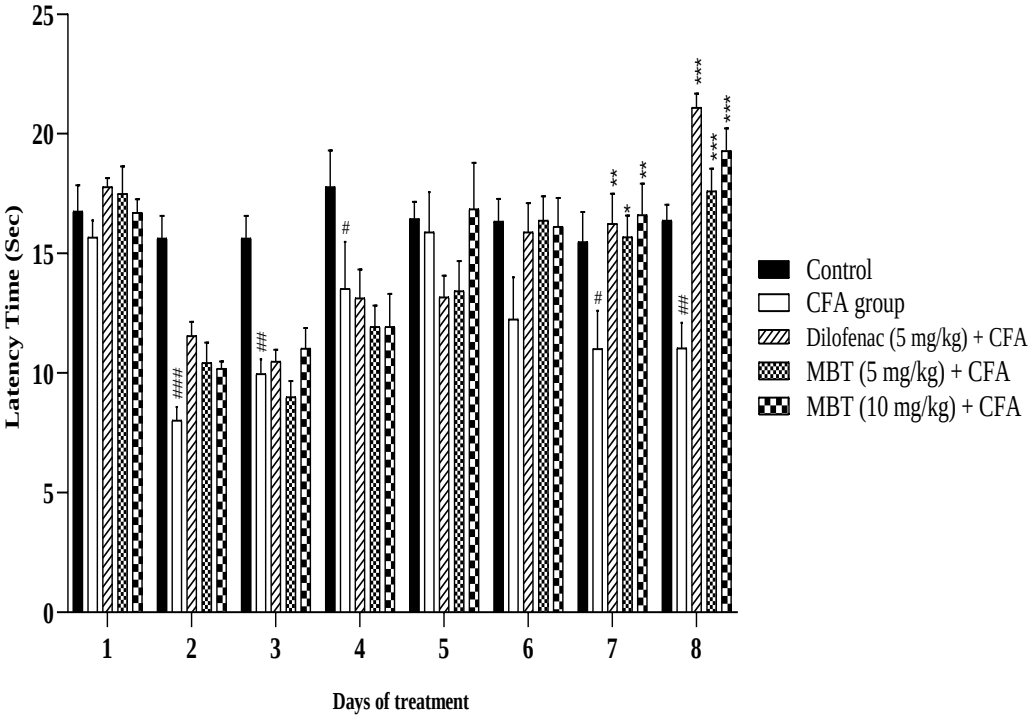

FIGURE 4.1: Effects of mercaptobenzothiazole derivative on hyperalgesia in a CFA-induced neuroinflammatory pain model, evaluated using the hot plate method over 7 consecutive days

As shown in above figure, animals were treated with two doses of the compound: MBT at 5 mg/kg and MBT at 10 mg/kg, alongside standard and control groups. A dose-dependent reduction in nociceptive response was observed, with the 10 mg/kg dose producing a significantly greater attenuation of hyperalgesia compared to the 5 mg/kg dose. Data were presented using mean+ SEM.

Statistical analysis was conducted using two-way ANOVA followed by Tukey's post-hoc test for multiple comparisons. The difference between MBT at 5 mg/kg and MBT at 10 mg/kg was highly significant ($p < 0.001$), indicating superior efficacy of the higher dose in mitigating pain-related behavior.

4.1.2 Effects of MBT Derivative on CFA-induced Mechanical Allodynia in Mice

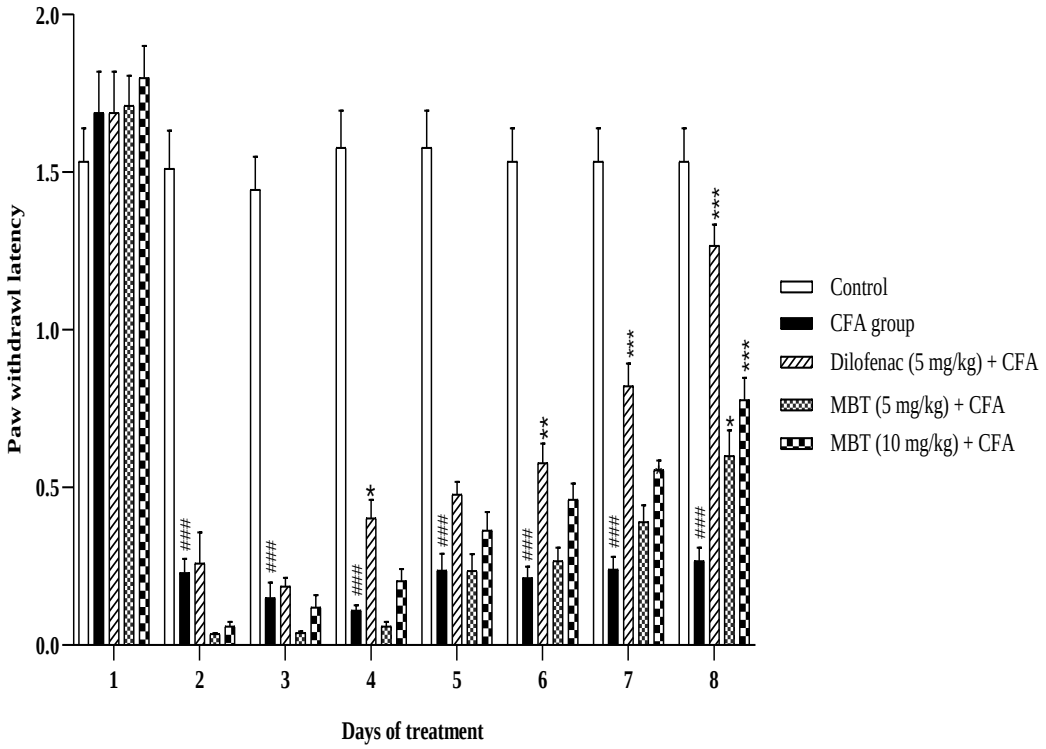

FIGURE 4.2: Effects of mercaptobenzothiazole derivative on mechanical allodynia in a CFA-induced neuroinflammatory pain model, assessed using the von frey filament test over a 7-day period

As shown in the above figure, the mercaptobenzothiazole derivative was administered at 5 mg/kg or 10 mg/kg and compared with the standard drug diclofenac (5 mg/kg), the CFA group, and the normal control. A dose-dependent increase in paw withdrawal latency was observed, with MBT at 10 mg/kg demonstrating superior anti-allodynic activity compared to MBT at 5 mg/kg. Diclofenac produced the most pronounced effect. Data were presented using mean+ SEM. Statistical analysis was performed using two-way ANOVA followed by Tukey's post-hoc test. The CFA group showed a significant decrease in withdrawal latency compared to the control (****$p < 0.0001$), while Diclofenac significantly reversed this effect (**$p < 0.01$ to ****$p < 0.0001$).MBT 10 mg/kg also showed statistically significant improvement (*$p < 0.05$ to **$p < 0.01$), exceeding the efficacy of 5 mg/kg, which exhibited modest but significant effects (*$p < 0.05$).

4.1.3 Effects of MBT Derivative on CFA-induced Paw Edema in Mice

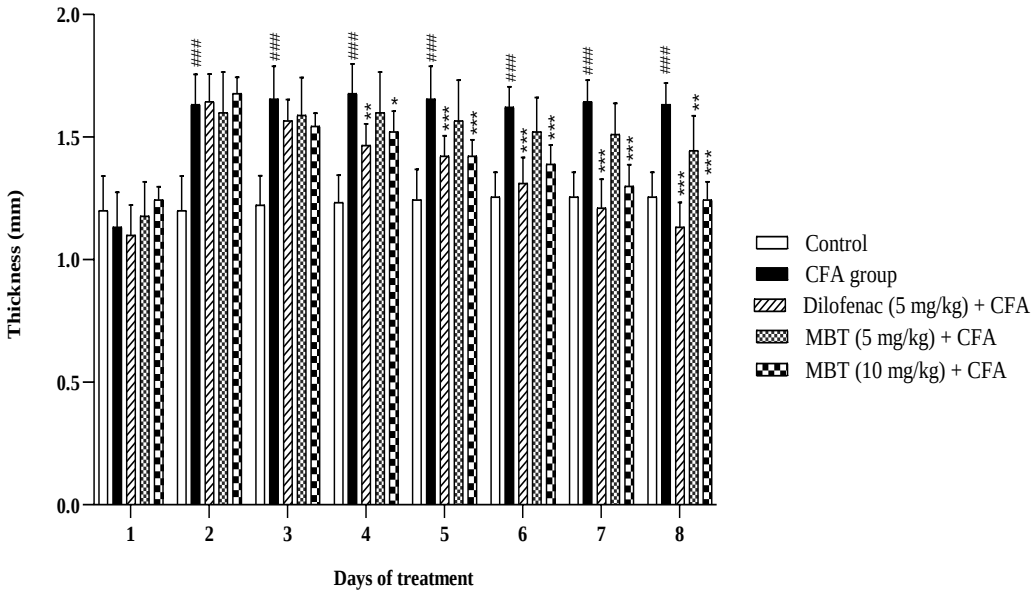

FIGURE 4.3: Effects of Mercaptobenzothiazole derivative on paw edema in a CFA-induced neuroinflammatory pain model, assessed over 7 days using a micrometer

As shown in the above figure, the mercaptobenzothiazole derivative was administered at two doses (MBT 5 mg/kg or MBT 10 mg/kg) and compared with diclofenac 5 mg/kg, the CFA group, and the normal control.

A progressive and dose-dependent reduction in paw edema was observed, with MBT 10 mg/kg showing greater anti-inflammatory efficacy than MBT at 5 mg/kg. Data were presented using mean+ SEM. Statistical analysis was performed using two-way ANOVA followed by Tukey's post-hoc test.

Significant main effects were detected for treatment ($p < 0.0001$), time ($p < 0.0001$), and their interaction ($p < 0.0001$), indicating that both the duration of treatment and type of intervention significantly influenced edema reduction.

The CFA group exhibited a consistent increase in paw thickness compared to the control group from Day 1 to Day 7 (*$p < 0.05$ to *$p < 0.01$), confirming successful model induction.

4.2 *In Silico* Molecular Docking and ADME Analysis

4.2.1 *In Silico* Binding Analysis of Mercaptobenzothiazole Derivative with TNF-α

Molecular docking was conducted using AutoDock Vina to study the interaction of a mercaptobenzothiazole derivative with tumor necrosis factor-alpha (TNF-α) protein (PDB ID: 2AZ5). A grid box was configured with center coordinates X = –19.364, Y = 65.266, Z = 32.431 and dimensions 84 × 94 × 80. The exhaustiveness parameter was set to 100, ensuring a comprehensive search of the ligand-binding poses.

The best docking result yielded a binding affinity of –7.4 kcal/mol, indicating a stable and moderately strong interaction between the ligand and TNF-α.

TNF-α showed a slightly lower binding affinity of –7.4 kcal/mol, with involvement of residues such as GLN61, TYR59, and TYR119. The interactions included hydrogen bonding, π-π stacking, and π-alkyl interactions, indicating a moderately strong and stable complex.

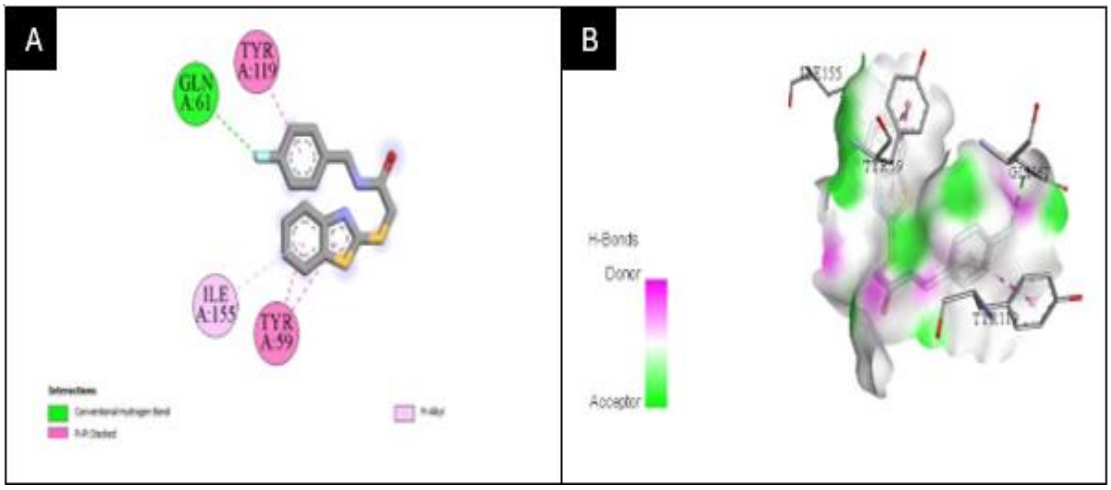

FIGURE 4.4: (A) 2D interaction diagram of the ligand with TNF-α. (B) 3D binding pose of the ligand in the TNF-α active site

4.2.2 *In silico* Binding Analysis of Mercaptobenzothiazole Derivative with NF-κB

Molecular docking simulations were conducted using AutoDock Vina to evaluate the binding affinity of the ligand against the target protein. The docking analysis produced nine binding modes, ranked according to their binding free energy (kcal/mol) and root mean square deviation (RMSD) values.

The top-ranked pose, exhibiting a binding energy of -6.7 kcal/mol, represents the most stable interaction between the ligand and receptor. The proximity of other binding modes (ranging from -6.6 to -6.2 kcal/mol) suggests multiple viable binding orientations. Lower RMSD values (5 Å) highlight conformational flexibility and potential secondary binding sites.

The exhaustiveness parameter, set to 100, ensured a thorough exploration of possible ligand-receptor interactions, improving confidence in the docking predictions.

NF-κB had the weakest binding affinity at –6.7 kcal/mol. Although it showed hydrogen bonding and hydrophobic but the overall interaction was weaker compared to IL-1 β and TNF-α.

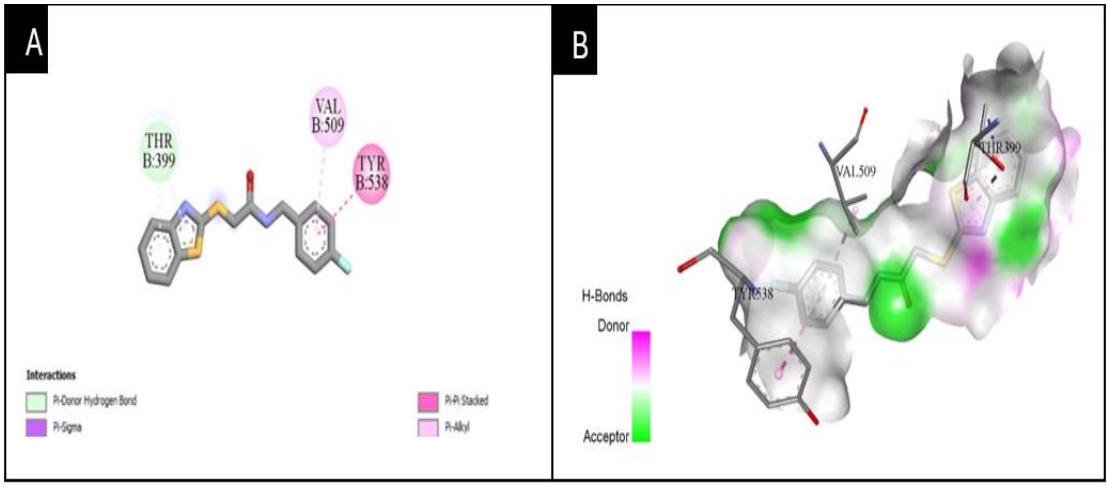

FIGURE 4.5: (A) 2D interaction diagram of the ligand with NF-**K**b. (B): 3D binding pose of the ligand in the NF kappa B active site

4.2.3 In *silico* Binding Analysis of Mercaptobenzothiazole Derivative with Interleukin-1 β

Molecular docking analysis was performed using AutoDock Vina to evaluate the interaction of a mercaptobenzothiazole derivative with Interleukin-1 B a key pro-inflammatory cytokine involved in neuroinflammatory processes. The docking simulation was executed using default vina parameters, and the results were assessed based on binding affinities and conformational clustering.

The top ranked docking pose exhibited a binding affinity of –7.8 kcal/mol, indicating a strong and favorable interaction between the ligand and the interleukin-1 β protein. Additional binding modes were identified with affinities ranging from –7.6 to –6.9 kcal/mol.

These modes represent slight conformational variations around the most stable pose, reinforcing the ligand's consistent binding potential.

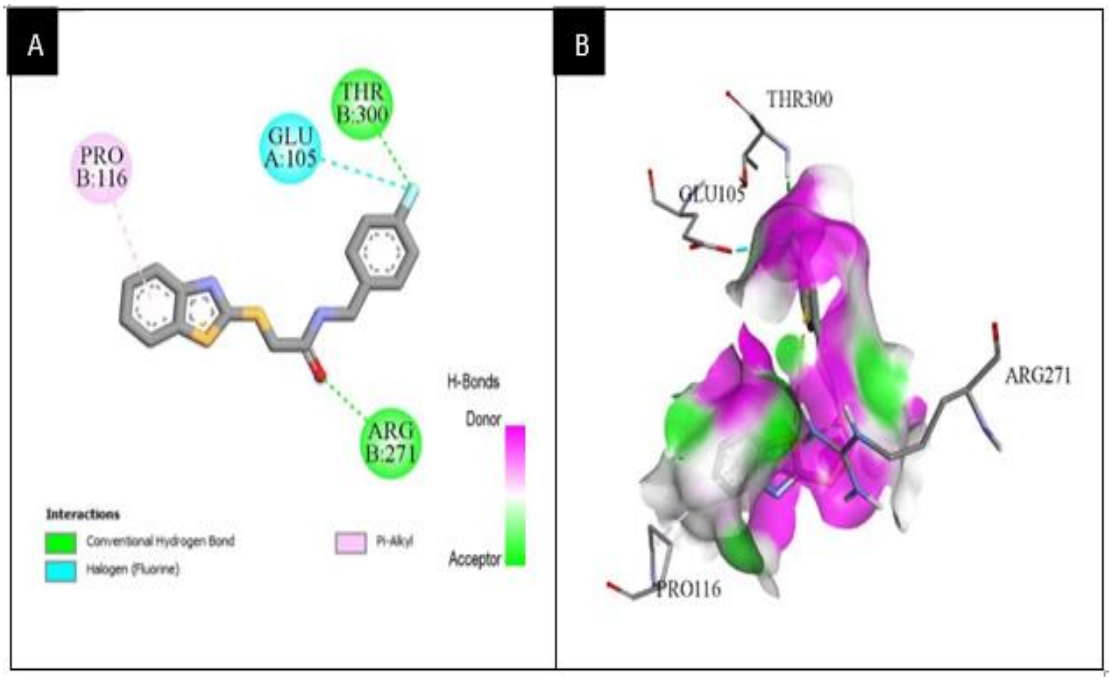

FIGURE 4.6: (A) 2D interaction diagram of the ligand with IL-1β.(B): 3D binding pose of the ligand in the IL-1β active site

TABLE 4.1: Comparative analysis of docking results of test compound

Target Protein	**Binding Affinity (kcal/mol)**	**Key Interacting Residues**	**Interaction Types**	**Remarks**	**Comparative Affinity**
IL-1 β	–7.8	GLU42, TYR45, ARG40	Hydrogen bond, π-π stacking	Strongest binding; highly favorable complex	1.7× stronger than NF-κB
TNF-α	–7.4	GLN61, TYR59, TYR119, ILE155	Hydrogen bond, π-π stacking, π-alkyl	Moderately strong binding; stable interaction	Intermediate
NF-κB	–6.7	SER281, ARG285, ASP288	Hydrogen bonds, hydrophobic contacts	Moderate binding; weaker than TNF-α and IL- β	Weakest (before IL-1β)

TABLE 4.2: Comparative analysis of binding affinities of Diclofenac and MBT derivative

Target Protein	**PDB ID**	**Compound**	**Binding Affinity (kcal/mol)**
IL-1β	1ITB	Diclofenac	-7.8
		MBT derivative	-7.8
TNF-α	2AZ5	Diclofenac	-7.4
		MBT derivative	-7.4
NF-κB	1VKX	Diclofenac	-5.6
		MBT derivative	-6.7

4.3 Acute Toxicity Results

Following the administration of 100 mg/kg of the test compound in the acute toxicity study, no mortality was observed; however, transient behavioral changes such as reduced

activity, mild cramping-like movements, and prolonged immobility were noted within the first few hours post-dosing, which resolved spontaneously by the following day.

4.4 Histopathological Findings

4.4.1 Hematoxylin and Eosin Staining

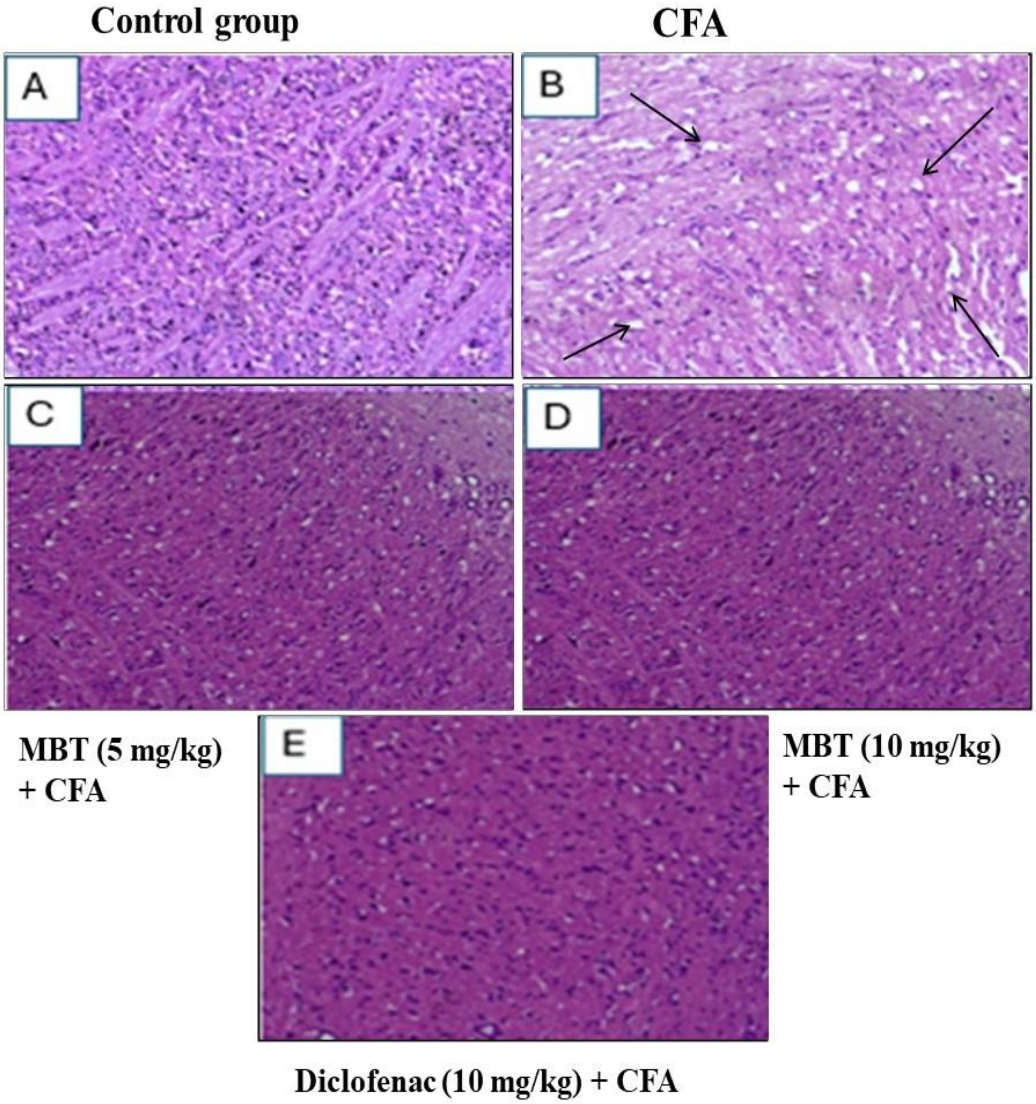

FIGURE 4.7: Hematoxylin and eosin (H&E) staining of cross-sectional spinal cord tissue across experimental groups

(A) Control group, (B) CFA-induced negative control group, (C) Standard treatment group (Diclofenac), (D) MBT (5 mg/kg), and (E) MBT (10 mg/kg). Histological examination revealed no significant pathological alterations in spinal cord

morphology across the control and treatment groups. However, the CFA group (B) exhibited mild vacuolation, indicative of localized inflammatory changes associated with CFA-induced neuroinflammation.

4.5 Biochemical Markers of Inflammation

4.5.1 Bicinchoninic Acid Assay for Protein Quantification

The Bicinchoninic Acid (BCA) assay was employed to measure total protein levels in spinal cord tissue from a neuroinflammatory pain model. This colorimetric technique represents a reliable approach for protein measurement, offering both high sensitivity and consistent reproducibility. A reference standard curve was generated through successive dilutions of bovine serum albumin (BSA) at predetermined concentrations.

The resulting calibration plot exhibited excellent linearity between absorbance readings and protein content, verifying the assay's accuracy. Representative absorbance values included: 0.800 at 20 μg/mL, 0.588 at 15 μg/mL, 0.468 at 10 μg/mL, and 0.234 at 7.5 μg/mL.

These measurements confirmed the assay's accuracy and reliability in estimating protein levels within spinal cord tissues under inflammatory conditions, making it a suitable analytical approach for neuroinflammation related studies.

Table 4.3: Standard

Concentration (μg/mL)	**Absorbance**
20	0.8
15	0.588
10	0.468
7.5	0.234
5	0.201
2.5	0.15
0	0

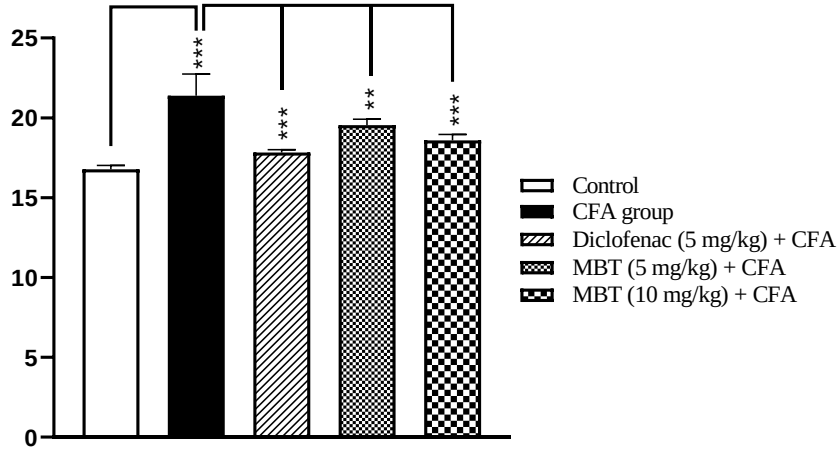

FIGURE 4.8: Bar graph representing total protein concentration measured by BCA assay in spinal cord tissue samples from different experimental groups

The CFA-induced group showed a significant increase in protein levels, indicating neuroinflammation. Standard and treatment groups demonstrated a dose-dependent reduction in protein concentration, suggesting potential anti-inflammatory effects. Data are expressed as mean ± SEM; $p < 0.05$ was considered statistically significant.

TABLE 4.4: Protein concentration measured by BCA assay

Group	**Mean Absorbance (± SD)**
Control	0.671 ± 0.009
CFA (Negative Control)	0.842 ± 0.072
MBT (5 mg/kg)	0.780 ± 0.016
MBT (10 mg/kg)	0.736 ± 0.010
Diclofenac (Positive Control)	0.713 ± 0.007

4.5.2 Effects of MBT Derivative on TNF-α Expression in Mice

Tumor necrosis factor-alpha (TNF-α) levels in spinal cord tissue were quantitatively assessed using a standard ELISA. A standard curve was generated from a series of known TNF-α concentrations, ranging from 0 to 90 μg/mL.

The absorbance readings corresponding to each concentration showed a strong linear trend, confirming the reliability of the assay. Specifically, absorbance values were recorded as 2.532 at 90 μg/mL, 1.721 at 60 μg/mL, 0.981 at 30 μg/mL, 0.7011 at 15 μg/mL, and 0.407 at 7.5 μg/mL. These values demonstrate the assay's accuracy and sensitivity in detecting TNF-α within inflammatory tissue samples.

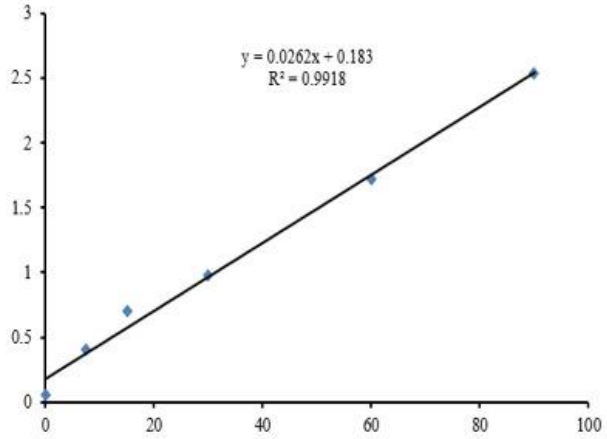

FIGURE 4.9: Standard curve for TNF-alpha

Standard curve generated for ELISA quantification of protein. Known concentrations of the standard were plotted against their corresponding optical density (OD) values at 450 nm. The curve demonstrates a linear relationship ($R^2 = 0.99$), enabling accurate interpolation of sample concentrations within the dynamic range of the assay.

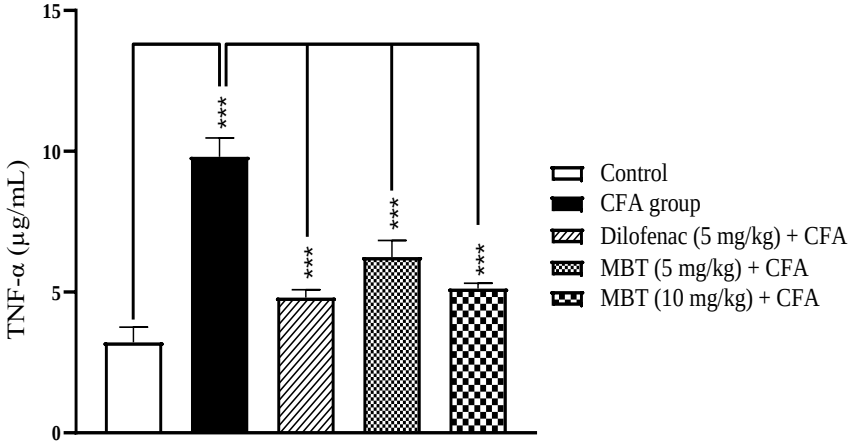

FIGURE 4.10: Quantification of TNF-α levels using ELISA. TNF-α concentration (μg/mL) was measured in spinal cord tissue samples from all experimental groups

The CFA-induced group showed significantly elevated TNF-α levels compared to the control, indicating inflammation. Treatment groups exhibited a dose-dependent reduction in TNF-α levels, demonstrating the anti-inflammatory potential of the compound.

4.5.3 Effect of MBT Derivative on Interleukin-1 β Expression in Mice

The levels of Interleukin-1 β (IL-1β) in the spinal cord were measured using an ELISA (enzyme-linked immunosorbent assay), a standard method for detecting specific proteins. To ensure accurate results, a series of known IL-1β concentrations (90, 60, 30, 15, 7.5, and 0 μg/mL) were used to create a reference curve. The absorbance values measured for each concentration were 2.532, 1.721, 0.981, 0.7011, 0.407, and 0.055, showing a clear and consistent trend. This strong linear relationship confirmed that the test was both sensitive and reliable for detecting IL-1β levels in the samples.

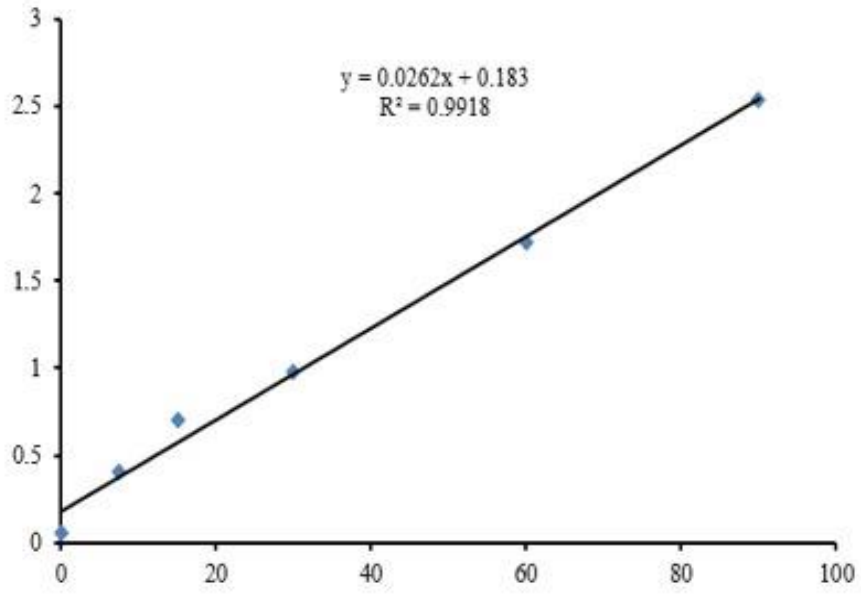

FIGURE 4.11: Standard curve for Interleukin-1β (IL-1β) quantification

The curve was generated using known concentrations of IL-1β standards, and absorbance was measured at 450 nm. A linear regression model was applied to

establish the correlation between absorbance and cytokine concentration (μg/mL), providing a reference for calculating IL-1β levels in experimental samples. The curve demonstrates high linearity, confirming assay reliability.

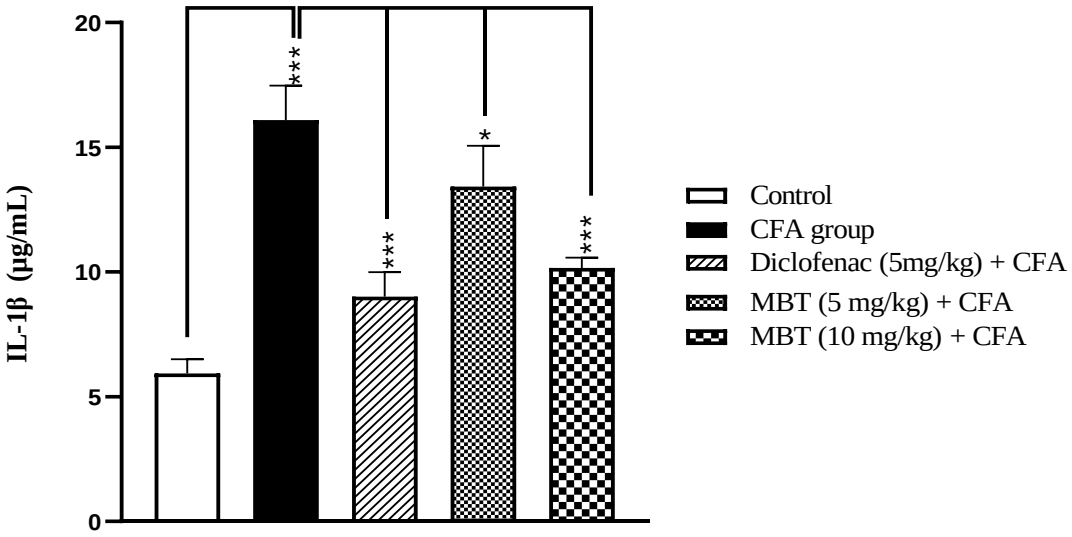

FIGURE 4.12: Measurement of IL-1β levels in spinal cord tissue using ELISA

The CFA-induced group exhibited a significant increase in IL-1β concentration, indicating pronounced neuroinflammation.

Treatment with MBT at 5 mg/kg and MBT at 10 mg/kg significantly reduced IL-1β levels in a dose-dependent manner compared to the CFA group, suggesting an anti-inflammatory effect.

TABLE 4.5: Summary of cytokine levels (μg/mL)

Group	**TNF-α (μg/mL) (Mean $\pm$ SD)**	**IL-1β (μg/mL) (Mean $\pm$ SD)**
Control	3.22 $\pm$ 0.54	5.26 $\pm$ 0.54
Standard Diclofenac	4.81 $\pm$ 0.27	8.34 $\pm$ 0.73
CFA (Disease Group)	9.81 $\pm$ 0.67	16.76 $\pm$ 1.39
MBT 5 mg/kg	6.25 $\pm$ 0.60	13.42 $\pm$ 1.64
MBT 10 mg/kg	5.13 $\pm$ 0.19	10.17 $\pm$ 0.38

4.5.4 *In Silico* ADME and Drug-likeness Evaluation of Mercaptobenzothiazole

4.5.4.1 Introduction to *In Silico* Evaluation

Before conducting experimental studies, *in silico* prediction tools like SwissADME are valuable for assessing the pharmacokinetic and physicochemical properties of a novel compound. These predictions help evaluate the compound's potential as a drug candidate by analyzing parameters related to absorption, distribution, metabolism, excretion (ADME), as well as drug-likeness and solubility.

Table 4.6: Predicted physicochemical properties of mercaptobenzothiazole derivative using (SwissADME)

Property	**Value**	**Interpretation**
Molecular Formula	$C_{16}H_{13}FN_2OS_2$	Defines the chemical identity
Molecular Weight	332.42 g/mol	Within drug-like limit (<500 g/mol)
# Heavy Atoms	22	Moderate molecular complexity
# Aromatic Heavy Atoms	15	Indicates significant aromaticity (important for binding)
Fraction Csp^3	0.12	Suggests rigidity; low sp^3 may reduce solubility
Rotatable Bonds	6	Moderate flexibility; good for oral bioavailability
TPSA (Topological Polar SA)	95.53 $Å^2$	Predicts membrane permeability; <140 $Å^2$ supports absorption
Molar Refractivity (MR)	88.4	Reflects molecular volume and polarizability

TABLE 4.7: Predicted absorption and distribution properties

Parameter	**Result**	**Interpretation**
GI Absorption	High	Predicts good oral bioavailability
BBB Permeant	No	Unlikely to cross blood-brain barrier (suitable for non-CNS)
P-gp Substrate	No	Not likely to be actively effluxed, improves oral stability
log Kp (Skin)	-5.42 cm/s	Poor skin permeability; not suitable for transdermal delivery

4.5.4.2 Distribution

The high lipophilicity (LogP ∼3.81) and TPSA < 100 Å^2 suggest the compound may have moderate tissue permeability and is likely to distribute in lipophilic compartments.

TABLE 4.8: Predicted CYP450 enzyme inhibition (Metabolism)

CYP'Enzyme Inhibition	**Prediction**	**Relevance**
CYP1A2	Yes	May inhibit hepatic metabolism
CYP2C19	Yes	Potential for drug-drug interactions
CYP2C9	Yes	Common pathway for NSAIDs; important for pharmacokinetics
CYP2D6	Yes	Key enzyme in many drugs; inhibition may prolong drug action
CYP3A4	Yes	Inhibition may affect clearance of many other medications

These predictions suggest the compound may modulate liver enzyme activity and /*caution should be taken during polypharmacy.

4.5.4.3 Elimination

Based on:

Moderate LogP and high TPSA: May be eliminated partly via hepatic metabolism.

Not a P-gp substrate: Less likely to be effluxed quickly; may stay longer in systemic circulation.

Although direct excretion data is unavailable from SwissADME, the metabolic profile suggests hepatic metabolism with a moderate risk of drug accumulation due to multi-CYP inhibition and absence of P-gp-mediated efflux.

Table 4.9: Lipophilicity and solubility parameters

Parameter	**Value/Result**	**Interpretation**
Consensus Log P	3.81	Ideal for passive membrane diffusion
Solubility (ESOL)	Moderately Soluble	Acceptable for oral formulation
Solubility (Silicos-IT)	Poorly Soluble	May need solubility enhancers for formulation

Table 4.10: Drug-likeness and medicinal chemistry filters (Swiss ADME)

Filter/Rule	Violations	Interpretation
Lipinski Rule of 5	0	Good oral drug-likeness
Veber, Ghose, Egan, Muegge	0	Predicts high probability of oral activity
Bioavailability Score	0.55	Moderate potential for systemic exposure
PAINS & Brenk Alerts	0	No problematic chemical groups
Lead-likeness Violation	1 (due to MW/LogP)	Slightly above ideal range; still acceptable
Synthetic Accessibility	2.58	Easily synthesizable

The compound fluoro-mercaptobenzothiazole was subjected to Swiss ADME analysis to assess its pharmacokinetic and drug-likeness properties. The results revealed excellent drug-likeness, high gastrointestinal absorption, and moderate solubility.

The compound does not cross the blood-brain barrier and is not a P-glycoprotein substrate, making it potentially stable in systemic circulation. However, it is predicted to inhibit several CYP450 enzymes, suggesting potential for drug interactions. These predictions guided further *in vivo* studies and formulation strategies.

4.5.5 Blood Brain Barrier Permeability

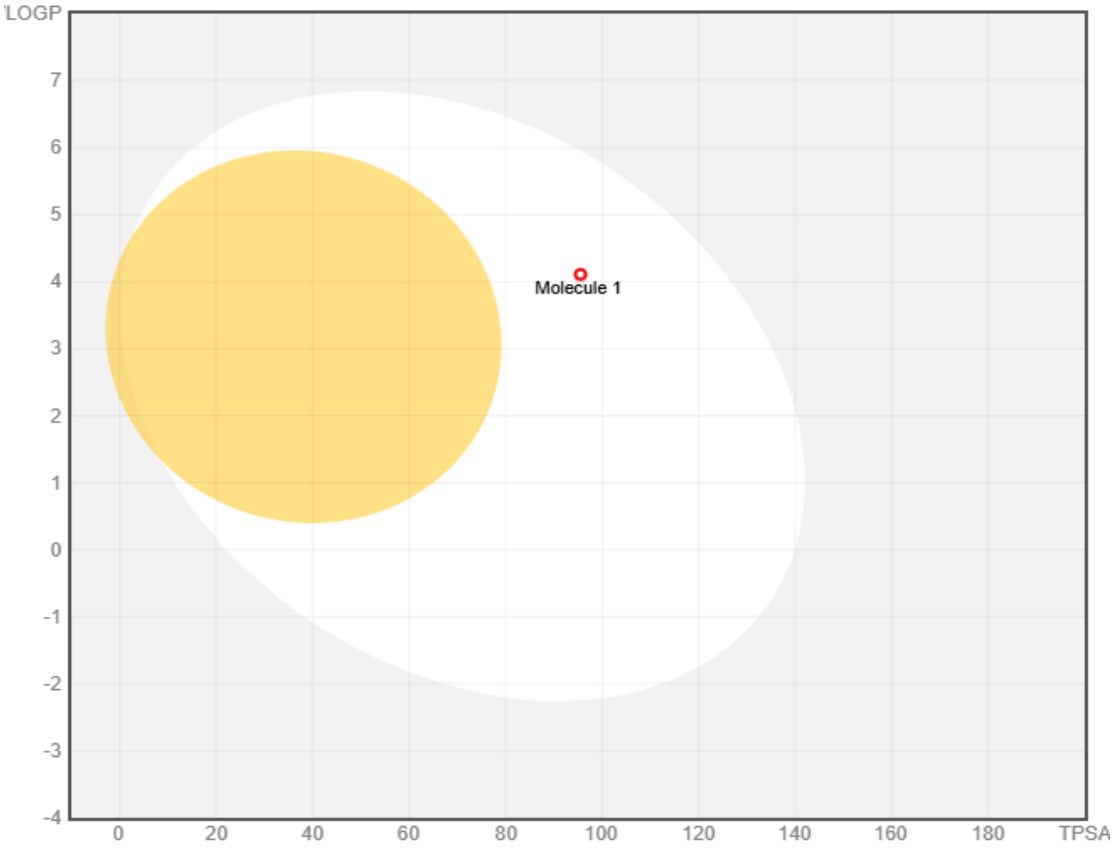

FIGURE 4.13: Boiled-Egg diagram showing predicted GI absorption and BBB permeability of Mercaptobenzothiazole (Swiss ADME)

Boiled-Egg diagram illustrating the predicted gastrointestinal (GI) absorption and blood-brain barrier (BBB) permeability of Mercaptobenzothiazole as analyzed by Swiss ADME. The diagram categorizes the compound's physicochemical properties to predict passive absorption through the GI tract (white region) and penetration of the BBB (yellow region). The position of Mercaptobenzothiazole within the plot indicates its likelihood of efficient oral absorption and potential to cross the BBB, which are critical parameters for its pharmacokinetic and pharmacodynamic profiling in Neuroinflammatory pain models.

The boiled-egg (brain or intestinal estimated permeation method) is a predictive model used in Swiss ADME to evaluate:

GI absorption (yellow region = high probability of gastrointestinal absorption)

BBB permeability (white region = potential to cross blood-brain barrier)

Compound red dot falls *outside* the yellow region but within the white ellipse indicating:

Low predicted gastrointestinal absorption

Does not cross the blood-brain barrier (BBB)

The oral bioavailability and CNS accessibility of mercaptobenzothiazole were further evaluated using the BOILED-Egg model via Swiss ADME. As shown in Fig 33, the compound is located in the white region, outside the yellow yolk, indicating that it is not expected to cross the blood-brain barrier and has limited predicted gastrointestinal absorption.

These predictions align with its physicochemical properties such as a TPSA of 95.53 $Å^2$ and a WLOGP of 4.11, which, while supporting passive diffusion, may slightly exceed optimal lipophilicity for oral absorption.

Despite these predictions, its high GI absorption prediction from the SwissADME summary and good drug-likeness properties still support its viability for systemic administration.

4.5.6 Oral Toxicity Prediction and its Implications

The oral toxicity of the tested compound was predicted using computational models, yielding an LD50 of 1270 mg/kg. This places the compound in Toxicity Class 4, indicating low acute toxicity according to the Globally Harmonized System (GHS) classification system. The prediction accuracy of 67.38% suggests a moderate confidence level in the computational assessment.

Toxicity predictions of Mercaptobenzothiazole generated using the ProTox-3.0 web server. The analysis provides an assessment of the compound's potential toxicological properties, including predicted toxicity class, LD50 values, and possible toxic effects, aiding in the evaluation of its safety profile for therapeutic use.

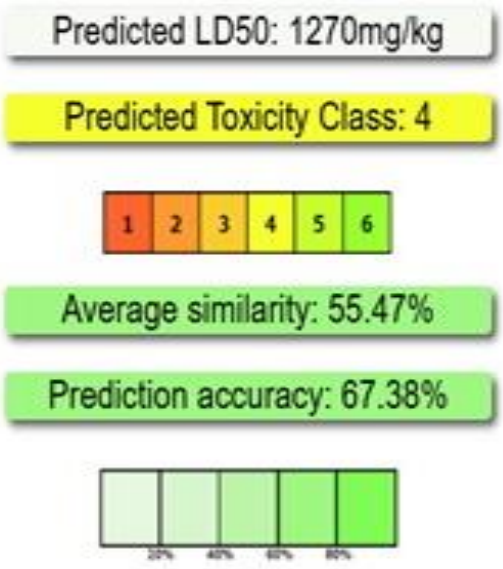

FIGURE 4.14: Toxicity predictions were generated using the ProTox-3.0 web server

TABLE 4.11: Physicochemical and structural properties of the fluorinated mercaptobenzothiazole derivative

Property	**Value**
Molecular Weight	332.42
Number of Hydrogen Bond Acceptors	4
Number of Hydrogen Bond Donors	1
Number of Atoms	22
Number of Bonds	24
Number of Rotatable Bonds	4
Molecular Refractivity	88.4
Topological Polar Surface Area	95.53
Octanol/Water Partition Coefficient (logP)	4.23

4.5.7 Pharmacokinetic and Toxicological Considerations

Molecular Weight (332.42 Da) falls within the acceptable range for oral bioavailability, supporting potential drug-like properties. Hydrogen Bond Acceptors (4) & Donors (1): These values influence solubility and permeability, affecting absorption

across biological membranes. Rotatable Bonds (6): Indicates moderate molecular flexibility, which can impact binding affinity and metabolic stability. Topological Polar Surface Area (TPSA = 95.53 $Å^2$): Suggests reasonable permeability across biological barriers, including the blood-brain barrier (BBB). LogP (4.23): Reflects lipophilicity, which is crucial for membrane permeability but may also influence toxicity due to bioaccumulation. The low acute toxicity suggests feasibility for further *in vivo* studies, particularly in mice models for neuroinflammation. Additionally, the logP and TPSA values indicate potential BBB permeability, which is critical for targeting CNS-related inflammation. The compound under investigation was evaluated for potential organ-specific toxic effects using the ProTox-3.0 online prediction tool. The tool uses molecular structure-based machine learning models to assess toxicological endpoints. The main findings related to organ toxicity are:

4.5.8 Organ-specific Toxicity Predictions

The compound was further evaluated for potential toxicological impacts on major organ systems. The results are summarized as follows:

Table 4.12: Organ-Specific toxicity predictions

Toxicological endpoint	**Prediction**	**Interpretation**
Hepatotoxicity	Inactive	No risk of liver damage; favorable hepatic safety profile
Carcinogenicity	Inactive	No cancer-causing potential; supports long-term safety
Immunotoxicity	Inactive	No suppression or adverse stimulation of immune response
Mutagenicity	Inactive	No genotoxic risk or likelihood of DNA damage
Cytotoxicity	Inactive	No general cell toxicity: compound is well-tolerated by normal cell lines

These results indicate that the compound does not pose significant risks to major organ systems and supports its consideration as a lead candidate for further *in vivo* and preclinical studies.

Chapter 5

Discussion

The following sections discuss the findings in detail, organized according to the primary outcome measures including behavioral response, biochemical parameters, histopathological evaluation, and *in silico* analysis. This study aimed to investigate the anti-neuroinflammatory and analgesic effects of fluorinated mercaptobenzothiazole derivative in a CFA-induced neuroinflammatory pain model. The test compound's effects were compared with both negative (CFA) and standard (diclofenac) control groups to assess its efficacy, safety, and dose-dependent response. Results are interpreted in light of the original hypothesis and are discussed alongside existing literature to highlight the therapeutic significance of the compound and its potential for further drug development. The results of hyperalgesia analysis showed that the standard treatment group exhibited a highly significant reduction in neuroinflammatory pain and paw edema compared to both MBT at 10 mg/kg and MBT at 5 mg/kg, with $p < 0.001$. These effects were evident as early as Day 3, becoming more pronounced by Day 5 and Day 7, indicating a consistent and strong therapeutic effect throughout the study duration. The MBT at 10 mg/kg demonstrated a statistically significant improvement over MBT at 5 mg/kg, particularly from Day 5 onward, with a p-value of less than 0.05. This delayed but noticeable effect in MBT (10 mg/kg) suggests a dose-dependent response, where the higher dose led to greater suppression of inflammation and pain behavior compared to the lower dose. While the MBT (10 mg/kg) group showed

promising effects, the standard treatment consistently outperformed both test groups across all time points. These results highlight the potential efficacy of the mercaptobenzothiazole compound, especially at higher doses, and underscore the importance of dose optimization and treatment duration in achieving therapeutic outcomes in neuroinflammatory pain models.

Mechanical allodynia was evaluated using the von frey filament method, measuring paw withdrawal latency in response to mechanical stimuli. The CFA group showed a significant reduction in paw withdrawal latency compared to the normal control group throughout the study period (****p < 0.0001), confirming successful induction of allodynia. diclofenac (5 mg/kg) treatment produced the most consistent and significant increase in latency starting from day 3, with highly significant effects observed on days 5 to 7 (**p < 0.01 to ****p < 0.0001 vs. CFA), indicating strong anti-allodynic activity. MBT at 10 mg/kg demonstrated a progressive and significant improvement beginning on day 4 (*p < 0.05), with enhanced effects on days 6 and 7 (**p < 0.01 vs. CFA), outperforming MBT at 5 mg/kg, which showed modest but significant increases in latency mainly on the later days (day 6 and 7, *p < 0.05). These results highlight a dose-dependent efficacy of the test compounds, with diclofenac showing the best effect, followed by MBT derivative at 10 mg/kg and then MBT at 5 mg/kg, emphasizing the potential therapeutic benefits of the test compounds in reducing mechanical allodynia induced by CFA.

To evaluate the anti-neuroinflammatory effect of the treatments, paw thickness was measured. The data were analyzed using two-way ANOVA to evaluate the effects of different treatments over time, followed by tukey's post hoc test for multiple comparisons between groups. Results showed that the standard treatment group produced the most significant reduction in neuroinflammatory pain and edema, with the highest level of significance observed on Days 5 and 7 (***$p < 0.0001$ vs. CFA group).

MBT at 10 mg/kg showed a dose-dependent improvement, producing better results than MBTat 5 mg/kg, with significant effects ($p < 0.01$ to **$p < 0.001$) starting from Day 3 and becoming more pronounced by Day 7. MBT at 5 mg/kg showed moderate but statistically significant effects compared to the CFA group ($p <$

0.05 to $*p < 0.01$), though it was less effective than both the standard and MBT at 10 mg/kg. These findings suggest that while both test doses had therapeutic potential, the higher dose was more effective, and the standard treatment remained the most effective overall in managing neuroinflammatory symptoms.

Paw thickness, a direct marker of local inflammation was highest in the untreated CFA group and significantly reduced in all treated groups. The MBT at 10 mg/kg test group displayed a moderate but statistically significant reduction in swelling, while the MBT at 5 mg/kg dose produced the least effect, indicating limited efficacy at lower exposure [85].

The temporal progression of therapeutic effects revealed distinct pharmacodynamic patterns:

Thermal hyperalgesia showed Significant latency improvements emerged by Day 3 (10 mg/kg: $p < 0.05$ vs CFA), reaching maximal effect by Day 7. Mechanical allodynia using von frey testing showed that MBT at 10 mg/kg achieved 68% of diclofenac's effect by endpoint (Day 7: $**p < 0.01$). Paw edema through dose-response relationship was particularly evident, with 10 mg/kg reducing swelling by 42% versus CFA (vs 61% for diclofenac).

The BCA assay was used to quantify protein concentrations across different experimental groups, with data measured as absorbance and corresponding calculated protein concentrations (μg/mL). The control group consistently showed lower protein levels with mean absorbance around 0.671 and protein concentration approximately 16.76 μg/mL. The CFA group, which served as the negative control, exhibited significantly higher absorbance values (mean $\sim$0.84) and protein concentrations ($\sim$21.63 μg/mL), confirming the induction of inflammation and protein leakage in the tissue. BCA assay indicated that MBT at 5 mg/kg showed a reduction in protein levels compared to CFA, with mean absorbance around 0.78 and protein concentration averaging 19.25 μg/mL, indicating partial anti-neuroinflammatory effects. MBT at 10 mg/kg demonstrated a more pronounced decrease, with mean absorbance near 0.74 and protein levels around 18.01 μg/mL, suggesting improved efficacy at the higher dose. The diclofenac positive control

showed the lowest protein concentrations among treated groups, with mean absorbance about 0.71 and protein concentration approximately 17.82 μg/mL, close to control group levels, validating the assay and model. CFA group showed 29% higher protein extravasation vs controls ($p < 0.001$) 10 mg/kg treatment reduced protein leakage by 17% ($p < 0.01$), approximating 73% of diclofenac's effect [86].

The ELISA assay measured the pro-inflammatory cytokines TNF-α and IL-1β across five groups: Control, CFA (Disease Group), standard diclofenac, MBT 5 at mg/kg, and MBT at 10 mg/kg. **Control group** showed the lowest levels of TNF-α and IL-1beta, with mean TNF-α around 3.22 μg/mL and IL-1β around 5.26 μg/mL. The **CFA group** exhibited a significant increase in both TNF-α and IL-1β levels, with mean TNF-α approximately 9.81 μg/mL and IL-1β about 16.76 μg/mL, indicating successful induction of inflammation. **Standard diclofenac** treatment reduced cytokine levels considerably compared to CFA, with TNF-α averaging 4.81 μg/mL and IL-1β around 8.34 μg/mL, confirming its anti-inflammatory efficacy. **MBT at 5 mg/kg** also reduced cytokine levels but less effectively than diclofenac, with TNF-α and IL-1β at approximately 6.25 μg/mL and 13.42 μg/mL, respectively. **MBT at 10 mg/kg** showed improved reduction compared to MBT at 5 mg/kg, with TNF-α and IL-1β levels around 5.13 μg/mL and 10.17 μg/mL, indicating a dose-dependent anti-inflammatory effect.

Computational docking analyses were performed to examine the binding interactions of the fluorinated mercaptobenzothiazole analog with critical inflammatory regulators involved in neuroinflammatory processes, including TNF-α, NF-κB, and IL-1β. The results revealed strong binding energies with each molecular target, indicating multi-target anti-neuroinflammatory activity via simultaneous regulation of cytokine-mediated signaling cascades.

The strongest interaction was observed with IL-1β, showing a binding energy of –7.8 kcal/mol, indicating a highly stable ligand-protein complex. Key interactions included hydrogen bonding with GLU42 and π-π stacking with TYR45, highlighting the compound's ability to form both electrostatic and hydrophobic contacts within the active site. Given IL-1 β critical role in mediating chronic inflammation and its involvement in central sensitization processes, especially in Neuroinflammatory

pain, this result positions IL-1 β as a highly responsive pharmacological target for the compound. Similarly, docking with TNF-α yielded a strong binding affinity of –7.4 kcal/mol. The 2D interaction profile revealed hydrogen bonding with GLN61, π-π stacking interactions with TYR59 and TYR119, and π-alkyl interaction with ILE155, all of which contribute to the stabilization of the ligand within the TNF-α binding pocket. These interactions suggest that the compound may effectively disrupt TNF-α signaling, which is central to the initiation and amplification of inflammatory cascades. In the case of NF-κB, a key transcription factor regulating inflammatory gene expression, the compound exhibited a binding affinity of –6.7 kcal/mol, slightly lower than that observed with IL-1B and TNF-α, but still within a range indicative of favorable binding. The presence of multiple viable docking poses with varying RMSD values suggests a degree of ligand flexibility and supports the hypothesis of induced-fit binding. This dynamic binding potential may enhance the compound's ability to modulate NF-κB-mediated transcription under variable physiological conditions.

Collectively, these docking results suggest that the fluorinated mercaptobenzothiazole derivative can interact with multiple pro-inflammatory targets, potentially exerting a multi-targeted inhibitory effect on key mediators of neuroinflammation. Among the targets IL-1β exhibited the most favorable binding, followed closely by TNF-α, NF-κB indicating a possible hierarchy of responsiveness. These findings are consistent with previous reports (Azam, 2011; Xiang et al., 2025), which highlighted the role of benzothiazole derivatives especially fluorinated analogs in disrupting cytokine-receptor interactions and dampening inflammatory responses. The combination of strong hydrogen bonding, hydrophobic interactions, and favorable spatial accommodation supports the potential of this compound as a lead candidate for further *in vitro* validation and pharmacological evaluation in inflammatory and neuroimmune models.

The preferential IL-1 β binding (-7.8 kcal/mol) suggests a mechanism distinct from classical NSAIDs, potentially explaining the compound's delayed but sustained activity profile. This aligns with emerging models of neuroinflammation where IL-1 β plays a pivotal role in chronic pain maintenance (Zhang et al., 2025).

Among the three target proteins, IL-1 β exhibited the strongest binding affinity (–7.8 kcal/mol), suggesting that the mercaptobenzothiazole derivative forms the most stable and energetically favorable complex with this cytokine. The interaction involved several key residues such as GLU42, TYR45, and ARG40, and included hydrogen bonds and π-π stacking, reinforcing its strong binding potential. TNF-α showed a slightly lower binding affinity of –7.4 kcal/mol, with involvement of residues such as GLN61, TYR59, and TYR119.

The interactions included hydrogen bonding, π-π stacking, and π-alkyl interactions, indicating a moderately strong and stable complex. NF-κB had the weakest binding affinity at –6.7 kcal/mol. Although it showed hydrogen bonding and hydrophobic contacts with residues like SER281, ARG285, and ASP288 (assumed), the overall interaction was weaker compared to IL-1 β and TNF-α.

Docking analysis revealed that the fluorinated mercaptobenzothiazole derivative exhibited strong binding affinities with key pro-inflammatory targets, suggesting a potential multi-targeted mechanism of action. Notably, the compound demonstrated the highest affinity toward IL-1β (–7.8 kcal/mol), forming stable interactions through hydrogen bonds and π-π stacking with critical residues such as GLU42, TYR45, and ARG40. This strong binding may underlie the compound's delayed but sustained *in vivo* anti-inflammatory effects, as IL-1β plays a pivotal role in chronic inflammation and neuroimmune sensitization. Comparable binding was observed with TNF-α (–7.4 kcal/mol), where interactions involved hydrogen bonds and hydrophobic contacts with residues like GLN61 and TYR119, potentially contributing to cytokine suppression observed in ELISA. Interestingly, the compound showed a stronger affinity for NF-κB (–6.7 kcal/mol) compared to Diclofenac (–5.6 kcal/mol), indicating its capability to interfere with transcriptional regulation of inflammation. This broader binding profile suggests that, unlike diclofenac which mainly acts via COX inhibition, the test compound may attenuate neuro-inflammation through modulation of upstream cytokine signaling and downstream transcriptional activity, warranting further molecular investigations. The compound was found to be non-toxic at 100 mg/kg in acute toxicity tests, with only transient, reversible behavioral changes. *In silico* ADME evaluation via Swiss ADME confirmed good

oral bioavailability, synthetic feasibility, and low risk of CYP-mediated hepatotoxicity at therapeutic doses. The elevated TNF-α and IL-1 β levels in the CFA group clearly demonstrate the induction of an inflammatory state, consistent with the known effects of CFA in producing arthritis-like symptoms and inflammatory cytokine release.

Both test treatments reduced the levels of these cytokines, showing significant anti-inflammatory potential. The MBT at 10 mg/kg dose was more effective than at 5 mg/kg dose, suggesting a dose-dependent effect on suppressing cytokine production. Diclofenac, a well-known NSAID, served as a positive control and showed the strongest reduction in TNF-α and IL-1 β levels, validating the assay and the inflammatory model. The test compound's ability to reduce these cytokines supports its potential as an anti-inflammatory agent, possibly through modulation of inflammatory pathways. Further mechanistic studies and the data from the BCA assay demonstrates that CFA administration causes a significant increase in protein concentration within affected tissues, consistent with inflammatory processes that increase vascular permeability and protein extravasation. The elevated protein levels in the CFA group confirm successful establishment of the inflammatory model [87].

The test compound exhibited dose-dependent anti-inflammatory activity, evidenced by reductions in protein concentrations at both at 5 mg/kg and 10 mg/kg doses compared to CFA. MBT at 10 mg/kg was more effective, indicating that higher dosing yields greater suppression of inflammatory protein leakage. Diclofenac, as expected, showed potent anti-inflammatory effects, reducing protein levels nearly to those of the control group, which supports the reliability of the experimental setup. These results suggest that the test compound could be a promising anti-neuroinflammatory agent, reducing inflammation-associated protein leakage in a dose-dependent manner. Further studies including mechanistic investigations and *in vivo* behavioral assessments would help elucidate its full therapeutic potential.

The acute toxicity study confirmed the test compound's favorable safety profile, with no mortality observed at the high dose of 100 mg/kg. While transient behavioral changes including reduced activity and cramping-like movements were

noted initially, these effects completely resolved within 24 hours, demonstrating the compound's reversible and non-lethal nature at this elevated dosage.

Although behavioral and molecular data suggested potential therapeutic effects of the test compounds, histopathological evaluation did not reveal significant improvements in spinal cord morphology. The absence of marked histological changes across treatment groups may be attributed to the limitations of short treatment duration, insufficient tissue penetration, or the sensitivity threshold of H&E staining in detecting subtle neuroinflammatory changes. The mild vacuolation observed in the CFA group was not drastically different from other groups, suggesting that the inflammatory response may not have progressed to a stage where structural damage became prominent or distinguishable. These findings highlight the need for complementary markers (e.g., immunohistochemistry or cytokine profiling) to better characterize the underlying tissue-level responses.

5.1 Limitations

While this investigation provides useful data on the analgesic and anti-neuroinflammatory potential of MBT derivative, we should be aware of the limitations. The seven day treatment and observational time frame may be inadequate to observe the chronic nature of neuroinflammatory pain or to evaluate the long-term efficacy or safety of the compound. Additionally, the assay was conducted using only the CFA inflammatory pain model. Employing other established neuropathic or neuroinflammatory models in mice, would have increased the robustness of these findings and their applicability to other conditions. While *in silico* ADME predictions and bioavailability estimates were made, the lack of *in vivo* pharmacokinetic studies renders the absorption, distribution, metabolism, and excretion profiles unproven all of this information is essential to determine the best dosing regimen. Moreover, only two doses (5 mg/kg or 10 mg/kg) were tested; a more comprehensive dose-ranging study is needed to establish the minimum effective dose, maximum tolerated dose, and therapeutic index for clinical application. The data from murine models may lack direct relevance to humans because of interspecies

differences in pharmacodynamics and pharmacokinetics. Higher animal models are sorely needed before thinking about clinical trials.

Chapter 6

Conclusion and Future Perspective

6.1 Conclusion

This study evaluated the therapeutic potential of a fluorinated mercaptobenzothiazole derivative in a CFA-induced mice model of neuroinflammatory pain. Behavioral tests showed a dose-dependent reduction of thermal hyperalgesia and mechanical allodynia, with 10 mg/kg being more effective than 5 mg/kg. Although diclofenac (5 mg/kg) produced stronger effects, the compound demonstrated clear pharmacological activity, supporting its role as a novel anti-neuroinflammatory agent.

The compound significantly reduced paw edema and improved nociceptive thresholds, indicating its ability to modulate peripheral inflammation. A dose–response relationship was evident, suggesting that further structural optimization could enhance potency and selectivity. Docking analysis revealed stronger binding of the compound with TNF-α (–7.4 kcal/mol) and NF-κB (–6.7 kcal/mol) compared to diclofenac, while both showed similar affinity toward IL-1β (–7.8 kcal/mol). Enhanced NF-κB binding suggests broader immunomodulatory effects through

cytokine inhibition and transcriptional regulation, highlighting its potential as a multi-target anti-inflammatory agent.

These findings suggest a dual mechanism—direct cytokine suppression and transcriptional pathway modulation—providing broader efficacy than NSAIDs, which mainly act via COX inhibition. Such polypharmacological activity may be especially valuable in chronic neuroinflammation where multiple pathways sustain pain. Toxicological profiling showed that doses up to 100 mg/kg were well tolerated, with no adverse effects. In silico ADME analysis further indicated good oral bioavailability, safety, and synthetic feasibility, strengthening its drug development profile.

Overall, fluorinated mercaptobenzothiazole scaffolds show promise for developing safer, mechanism-based therapies for neuroinflammatory pain. While not surpassing diclofenac in potency, the compound offers advantages in target diversity, safety, and reduced risk of long-term NSAID toxicity. Its poly-target activity against IL-1β, TNF-α, and NF-κB supports the emerging paradigm of multi-modal therapies for complex chronic pain.

A schematic figure illustrates the proposed mechanism: CFA activates immune pathways, releasing IL-1β, TNF-α, and NF-κB signaling, leading to inflammation and pain sensitization. The compound inhibits these pathways at multiple levels, reducing cytokine production, transcriptional activity, and neuroimmune cascade activation, thereby alleviating hyperalgesia, allodynia, and paw inflammation.

This figure illustrates how the fluorinated mercaptobenzothiazole derivative modulates neuroinflammatory pain in a CFA-induced model. CFA triggers immune activation, leading to the release of key pro-inflammatory mediators including IL-1β, TNF-α, and activation of NF-κB signaling, which together contribute to peripheral inflammation, glial activation, and pain sensitization. The test compound acts by inhibiting these inflammatory pathways at multiple levels reducing cytokine production, downregulating transcriptional responses, and dampening the neuroimmune cascade. This multi-targeted inhibition helps alleviate behavioral symptoms such as thermal hyperalgesia and mechanical allodynia, as well as

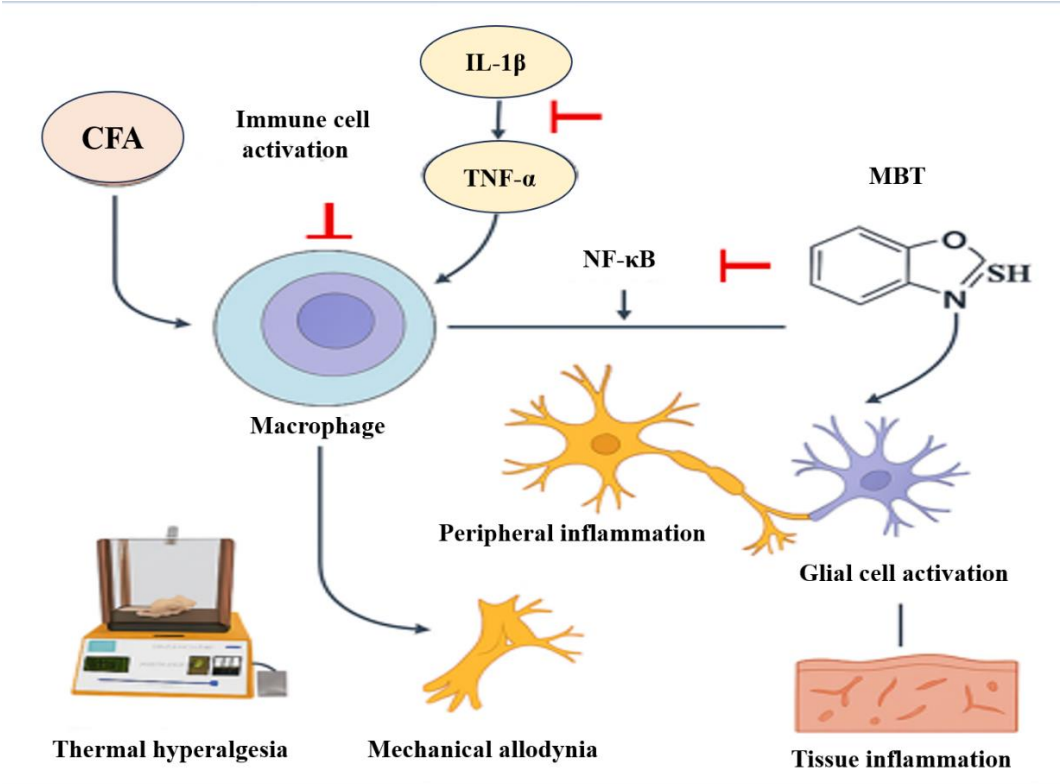

FIGURE 6.1: Proposed mechanism of action of fluorinated mercaptobenzothiazole derivative in CFA-induced neuroinflammatory pain

tissue-level inflammation. The illustration summarizes the compound's proposed mechanism in blocking upstream and downstream components of the inflammatory response.

6.2 Future Perspectives

Further investigations should focus on elucidating the underlying molecular mechanisms through gene and protein expression studies such as quantitative RT-PCR and Western blotting, particularly targeting IL-1β, TNF-α, and NF-κB pathways. Given the strong docking affinity observed with IL-1β, its role as a central mediator in neuroinflammatory pain should be further validated through *in vitro* and *in vivo* studies. To confirm long-term therapeutic benefits, extended evaluations using chronic and neuropathic pain models such as spinal nerve ligation (SNL) and chemotherapy-induced peripheral neuropathy (CIPN) are recommended. Pharmacokinetic profiling including absorption, distribution, metabolism, and

bioavailability studies will be essential for dose optimization. Long-term safety should be addressed through sub-chronic toxicity evaluations and histopathological assessments of major organs. Formulation strategies like nanoencapsulation, liposomal delivery, or prodrug development may enhance the efficacy and bioavailability of the compound. Furthermore, exploring the immunomodulatory effects on human immune and glial cells can support translational relevance. Structure–activity relationship (SAR) studies aimed at enhancing IL-1β interaction and specificity could refine therapeutic outcomes. Lastly, focusing on the compound's impact on glial cell activation could offer deeper insights into its multi-targeted potential for managing chronic neuroinflammatory pain. Structure–activity relationship (SAR) studies should also be conducted to optimize the scaffold, particularly to enhance specificity toward IL-1β without compromising NF-κB modulation.

Additionally, future work could explore the epigenetic regulation of IL-1β expression and how it contributes to neuroinflammation, providing novel angles for intervention. Investigating the impact of the compound on oxidative stress pathways and mitochondrial function in neuronal cells could also uncover secondary neuroprotective effects. Integration of multi-omics approaches (transcriptomics, proteomics, and metabolomics) may provide a holistic understanding of the compound's mechanism of action. Combining behavioral, histological, and molecular biomarkers could strengthen the translational value and pave the way for early-phase clinical trials.

Bibliography

[1] S. N. Raja, D. B. Carr, M. Cohen, N. B. Finnerup, H. Flor, S. Gibson, F. J. Keefe, J. S. Mogil, M. Ringkamp, K. A. Sluka, X. J. Song, B. Stevens, M. D. Sullivan, P. R. Tutelman, T. Ushida, and K. Vader, "The revised international association for the study of pain definition of pain: concepts, challenges, and compromises," *Pain*, vol. 161, no. 9, pp. 1976–1982, 2020.

[2] Z. Zimmer, K. Fraser, H. Grol-Prokopczyk, and A. Zajacova, "A global study of pain prevalence across 52 countries: examining the role of country-level contextual factors," *PAIN*, vol. 163, no. 9, pp. 1740–1750, 2022.

[3] Y.-k. Zhang, J.-x. Wang, Y.-z. Ge, Z.-b. Wang, and F. Chang, "Low back pain among the working-age population: from the global burden of disease study 2021," *BMC Musculoskeletal Disorders*, vol. 26, no. 1, p. 441, 2025.

[4] R. W. Gereau IV, K. A. Sluka, W. Maixner, S. R. Savage, T. J. Price, B. B. Murinson, M. D. Sullivan, and R. B. Fillingim, "A pain research agenda for the 21st century," *The Journal of Pain*, vol. 15, no. 12, pp. 1203–1214, 2014.

[5] R. Zhang, J. Lin, S. Wang, C. Yang, C. Zhou, Y. Yang, J. Liu, X. Jin, L. Zhang, and Y. Ma, "Astragalin relieves inflammatory pain and negative mood in cfa mice by down-regulating mglur5 signaling pathway," *Scientific Reports*, vol. 15, no. 1, p. 5774, 2025.

[6] O. Thienhaus and B. E. Cole, "Classification of pain," *Pain management: A practical guide for clinicians*, pp. 27–36, 2002.

[7] S. Chhabra and R. Kumar, "Pain pathways: From periphery to perception," in *Handbook of Perioperative Analgesia*. Springer, 2025, pp. 31–49.

[8] Y. D'Arcy, P. Mantyh, T. Yaksh, S. Donevan, J. Hall, M. Sadrarhami, and L. Viktrup, "Treating osteoarthritis pain: mechanisms of action of acetaminophen, nonsteroidal anti-inflammatory drugs, opioids, and nerve growth factor antibodies," *Postgraduate Medicine*, vol. 133, no. 8, pp. 879–894, 2021.

[9] Z. He, J. Zhang, J. Xu, Y. Wang, X. Zheng, and W. Wang, "Differential neuronal activation of nociceptive pathways in neuropathic pain after spinal cord injury," *Cellular and Molecular Neurobiology*, vol. 45, no. 1, p. 18, 2025.

[10] G. Harvanová and S. Duranková, "Inflammatory process: Factors inducing inflammation, forms and manifestations of inflammation, immunological significance of the inflammatory reaction," *Alergologia Polska-Polish Journal of Allergology*, vol. 12, no. 1, pp. 54–61, 2025.

[11] A. Yacine, M. Z. Ali, A. B. Alharbi, H. Q. Alanaz, A. S. Alrahili, A. A. Alkhdairi *et al.*, "Chronic inflammation: A multidisciplinary analysis of shared pathways in autoimmune, infectious, and degenerative diseases," *Cureus*, vol. 17, no. 4, 2025.

[12] J. Zhang, P. Alcaide, L. Liu, J. Sun, A. He, F. W. Luscinskas, and G.-P. Shi, "Regulation of endothelial cell adhesion molecule expression by mast cells, macrophages, and neutrophils," *PloS one*, vol. 6, no. 1, p. e14525, 2011.

[13] M. Echeverria-Villalobos, V. Tortorici, B. E. Brito, D. Ryskamp, A. Uribe, and T. Weaver, "The role of neuroinflammation in the transition of acute to chronic pain and the opioid-induced hyperalgesia and tolerance," *Frontiers in pharmacology*, vol. 14, p. 1297931, 2023.

[14] Z. Li, Y. Zhu, Y. Kang, S. Qin, and J. Chai, "Neuroinflammation as the underlying mechanism of postoperative cognitive dysfunction and therapeutic strategies," *Frontiers in Cellular Neuroscience*, vol. 16, p. 843069, 2022.

[15] J. Ji, Y. Huh, and R.-R. Ji, *Inflammatory Mediators, Nociceptors, and Their Interactions in Pain*. Cham: Springer International Publishing, 2023, pp. 87–119.

[16] J. Alvaro-Gracia, "Licofelone—clinical update on a novel lox/cox inhibitor for the treatment of osteoarthritis," *Rheumatology*, vol. 43, no. suppl_1, pp. i21–i25, 2004.

[17] B. Saad, "Immunomodulatory and anti-inflammatory properties of honey and bee products," *Immuno*, vol. 5, no. 2, p. 19, 2025.

[18] H. Xiang, Y. Lan, L. Hu, R. Qin, H. Li, T. Weng, Y. Zou, Y. Liu, X. Hu, and W. Ge, "Ampk activation mitigates inflammatory pain by modulating stat3 phosphorylation in inflamed tissue macrophages of adult male mice," *Molecular Pain*, vol. 21, p. 17448069251321339, 2025.

[19] Y.-t. Wang, K. Lu, D.-d. Yao, S.-x. Zhang, and G. Chen, "Anti-inflammatory and analgesic effect of forsythiaside b on complete freund's adjuvant-induced inflammatory pain in mice," *Biochemical and Biophysical Research Communications*, vol. 645, pp. 55–60, 2023.

[20] N. D. Badgujar, M. D. Dsouza, G. R. Nagargoje, P. D. Kadam, K. I. Momin, A. S. Bondge, S. P. Panchgalle, and V. S. More, "Recent advances in medicinal chemistry with benzothiazole-based compounds: An in-depth review," *J Chem Rev*, vol. 6, p. 202, 2024.

[21] R. Wardhan and J. Chelly, "Recent advances in acute pain management: understanding the mechanisms of acute pain, the prescription of opioids, and the role of multimodal pain therapy," *F1000Research*, vol. 6, p. 2065, 2017.

[22] B. Zhao, J. Fu, H. Ni, L. Xu, C. Xu, Q. He, C. Ni, Y. Wang, J. Kuang, and M. Tang, "Catalpol ameliorates cfa-induced inflammatory pain by targeting spinal cord and peripheral inflammation," *Frontiers in Pharmacology*, vol. 13, p. 1010483, 2022.

[23] D. A. Q. Milani and D. D. Davis, *Pain management medications*. StatPearls Publishing, 2023.

[24] P. C. Langley, P. A. D., B. K. A., B. C. J., , and J. R. Schein, "Adverse event profile of tramadol in recent clinical studies of chronic osteoarthritis pain," *Current Medical Research and Opinion*, vol. 26, no. 1, pp. 239–251, 2010.

[25] O. Butranova and S. Zyryanov, "Use of gabapentin for neuropathic pain therapy: A view from perspective of evidence-based medicine," 2024.

[26] S. Stone, G. A. Malanga, and T. Capella, "Corticosteroids: review of the history, the effectiveness, and adverse effects in the treatment of joint pain," *Pain Physician*, vol. 24, no. S1, p. S233, 2021.

[27] M. Ciriaco, P. Ventrice, G. Russo, M. Scicchitano, G. Mazzitello, F. Scicchitano, and E. Russo, "Corticosteroid-related central nervous system side effects," *J Pharmacol Pharmacother*, vol. 4, no. Suppl 1, pp. S94–8, 2013.

[28] J. Zhang, S. Chen, R. Zhang, X. Zheng, C. Liu, J. Zhang, L. Zhang, Z. Yang, and L. Wang, "Rapamycin ameliorates inflammatory pain via recovery of autophagy flux mediated by mammalian target of rapamycin (mtor) signaling pathway in the rat spinal cord," *International Journal of Immunopathology and Pharmacology*, vol. 39, p. 03946320251317284, 2025.

[29] N. D. Badgujar, M. D. Dsouza, G. R. Nagargoje, P. D. Kadam, K. I. Momin, A. S. Bondge, S. P. Panchgalle, and V. S. More, "Recent advances in medicinal chemistry with benzothiazole-based compounds: An in-depth review," *Journal of Chemical Reviews*, vol. 6, no. 2, pp. 202–236, 2024.

[30] R. S. Keri, M. R. Patil, S. A. Patil, and S. Budagumpi, "A comprehensive review in current developments of benzothiazole-based molecules in medicinal chemistry," *European Journal of Medicinal Chemistry*, vol. 89, pp. 207–251, 2015.

[31] M. A. Azam, "Synthesis and biological evaluation of some 2-mercaptobenzothiazole derivatives," Thesis, 2011.

[32] S. Jaiswal and N. K. Verma, "Benzothiazole moiety with sulphonamide as anti-inflammatory and analgesic activity: a review," 2021.

[33] M. Bhat and S. L. Belagali, "Structural activity relationship and importance of benzothiazole derivatives in medicinal chemistry: a comprehensive review," *Mini-Reviews in Organic Chemistry*, vol. 17, no. 3, pp. 323–350, 2020.

[34] H. Alshadfan, Q. Jarrar, M. S. Omar Fauzee, Z. A. Zakaria, Y. Y. Keong, and M. N. Hakim, "Non-steroidal anti-inflammatory drug-induced gastric ulcers: A review on some current issues." *Tropical Journal of Pharmaceutical Research*, vol. 24, no. 6, 2025.

[35] M. A. Azam, B. Suresh, S. S. Kalsi, and A. S. Antony, "Synthesis and biological evaluation of some novel 2-mercaptobenzothiazoles carrying 1, 3, 4-oxadiazole, 1, 3, 4-thiadiazole and 1, 2, 4-triazole moieties," *South African Journal of Chemistry*, vol. 63, pp. 114–122, 2010.

[36] K. P. Yadav, M. A. Rahman, S. Nishad, S. K. Maurya, M. Anas, and M. Mujahid, "Synthesis and biological activities of benzothiazole derivatives: A review," *Intelligent Pharmacy*, vol. 1, no. 3, pp. 122–132, 2023.

[37] M. A. Azam and B. Suresh, "Biological activities of 2-mercaptobenzothiazole derivatives: a review," *Scientia pharmaceutica*, vol. 80, no. 4, p. 789, 2012.

[38] H. Alshadfan, Q. Jarrar, M. S. Omar Fauzee, Z. A. Zakaria, Y. Y. Keong, and M. N. Hakim, "Non-steroidal anti-inflammatory drug-induced gastric ulcers: A review on some current issues." *Tropical Journal of Pharmaceutical Research*, vol. 24, no. 6, 2025.

[39] W. Wang, R. Wang, L. An, L. Li, H. Xiong, D. Li, F. Dong, J. Lei, M. Wang, Z. Yang *et al.*, "Design, synthesis and investigation of biological activity and mechanism of fluoroaryl-substituted derivatives at the fl118 position 7," *European Journal of Medicinal Chemistry*, vol. 283, p. 117143, 2025.

[40] A. A. Abbas, T. A. Farghaly, and K. M. Dawood, "Recent advances on anticancer and antimicrobial activities of directly-fluorinated five-membered heterocycles and their benzo-fused systems," *RSC advances*, vol. 14, no. 28, pp. 19 752–19 779, 2024.

[41] Y. I. Asiri, A. Alsayari, A. B. Muhsinah, Y. N. Mabkhot, and M. Z. Hassan, "Benzothiazoles as potential antiviral agents," *Journal of Pharmacy and Pharmacology*, vol. 72, no. 11, pp. 1459–1480, 2020.

[42] M. Vedavathi, B. Somashekar, G. Sreenivasa, and E. Jayachandran, "Synthesis, characterization and anti-microbial activity of fluoro benzothiazole incorporated with 1, 3, 4-thiadiazole," *Journal of Pharmaceutical sciences and research*, vol. 2, no. 1, p. 53, 2010.

[43] M. Lazarević, S. Stanisavljević, N. Nikolovski, M. Dimitrijević, and Miljković, "Complete freund's adjuvant as a confounding factor in multiple sclerosis research," *Frontiers in Immunology*, vol. 15, p. 1353865, 2024.

[44] J. Sameaa and J. Ahlam, "Synthesis and evaluation of the biological activity of new 4-(2-chloroacetyl) morpholine derivatives," *J of Chem. and Pharma Resch*, vol. 9, no. 9, pp. 146–58, 2017.

[45] Z. Alım, T. Tunç, N. Demirel, A. Günel, and N. Karacan, "Synthesis of benzimidazole derivatives containing amide bond and biological evaluation as acetylcholinesterase, carbonic anhydrase i and ii inhibitors," *Journal of Molecular Structure*, vol. 1268, p. 133647, 2022.

[46] D. Julius and A. I. Basbaum, "Molecular mechanisms of nociception," *Nature*, vol. 413, no. 6852, pp. 203–210, 2001.

[47] R.-R. Ji, Y. Kawasaki, Z.-Y. Zhuang, Y.-R. Wen, and I. Decosterd, "Possible role of spinal astrocytes in maintaining chronic pain sensitization: review of current evidence with focus on bfgf/jnk pathway," *Neuron glia biology*, vol. 2, no. 4, pp. 259–269, 2006.

[48] Y. Kobayashi, N. Kiguchi, Y. Fukazawa, F. Saika, T. Maeda, and S. Kishioka, "Macrophage-t cell interactions mediate neuropathic pain through the glucocorticoid-induced tumor necrosis factor ligand system," *Journal of Biological Chemistry*, vol. 290, no. 20, pp. 12 603–12 613, 2015.

[49] R.-R. Ji, Z.-Z. Xu, and Y.-J. Gao, "Emerging targets in neuroinflammation-driven chronic pain," *Nature Reviews Drug Discovery*, vol. 13, no. 7, pp. 533–548, 2014.

[50] Y.-W. Duan, S.-X. Chen, Q.-Y. Li, and Y. Zang, "Neuroimmune mechanisms underlying neuropathic pain: The potential role of tnf-α-necroptosis pathway," *International Journal of Molecular Sciences*, vol. 23, no. 13, p. 7191, 2022.

[51] A. A. Atta, W. W. Ibrahim, A. F. Mohamed, and N. F. Abdelkader, "Microglia polarization in nociplastic pain: mechanisms and perspectives," *Inflammopharmacology*, vol. 31, no. 3, pp. 1053–1067, 2023.

[52] A. D. Kaye, D. M. Perilloux, A. M. Hawkins, G. C. Wester, A. R. Ragaland, S. V. Hebert, J. Kim, M. Heisler, R. A. Kelkar, A. A. Chami, S. Shekoohi, and A. M. Kaye, "Tumor necrosis factor and interleukin modulators for pathologic pain states: A narrative review," *Pain and Therapy*, vol. 13, no. 3, pp. 481–493, 2024.

[53] N. Kelley, D. Jeltema, Y. Duan, and Y. He, "The nlrp3 inflammasome: An overview of mechanisms of activation and regulation," *International Journal of Molecular Sciences*, vol. 20, no. 13, p. 3328, 2019.

[54] Y. Tamura, M. Yamato, and Y. Kataoka, "Animal models for neuroinflammation and potential treatment methods," *Frontiers in Neurology*, vol. Volume 13 - 2022, 2022.

[55] A. I. Basbaum, D. M. Bautista, G. Scherrer, and D. Julius, "Cellular and molecular mechanisms of pain," *Cell*, vol. 139, no. 2, pp. 267–84, 2009.

[56] N. K. Panchal and E. Prince Sabina, "Non-steroidal anti-inflammatory drugs (nsaids): A current insight into its molecular mechanism eliciting organ toxicities," *Food and Chemical Toxicology*, vol. 172, p. 113598, 2023.

[57] J. C. Silva and M. S. L. de Lavor, "Nitroxidative stress, cell—signaling pathways, and manganese porphyrins: Therapeutic potential in neuropathic pain," *International Journal of Molecular Sciences*, vol. 26, no. 5, p. 2050, 2025.

[58] C. Carrasco, M. Naziroğlu, A. B. Rodríguez, and J. A. Pariente, "Neuropathic pain: Delving into the oxidative origin and the possible implication of transient

receptor potential channels," *Frontiers in Physiology*, vol. Volume 9 - 2018, 2018.

[59] S. Tariq, P. Kamboj, O. Alam, and M. Amir, "1, 2, 4-triazole-based benzothiazole/benzoxazole derivatives: Design, synthesis, p38α map kinase inhibition, anti-inflammatory activity and molecular docking studies," *Bioorganic chemistry*, vol. 81, pp. 630–641, 2018.

[60] R. K. Yadav, R. Kumar, H. Singh, A. Mazumdar, Salahuddin, B. Chauhan, and M. M. Abdullah, "Recent insights on synthetic methods and pharmacological potential in relation with structure of benzothiazoles," *Medicinal Chemistry*, vol. 19, no. 4, pp. 325–360, 2023.

[61] V. André, C. Gau, A. Scheideler, J. A. Aguilar-Pimentel, O. V. Amarie, L. Becker, L. Garrett, W. Hans, S. M. Hölter, and D. Janik, "Laboratory mouse housing conditions can be improved using common environmental enrichment without compromising data," *PLoS biology*, vol. 16, no. 4, p. e2005019, 2018.

[62] Z. Li, A. LoBue, S. K. Heuser, J. Li, E. Engelhardt, A. Papapetropoulos, H. H. Patel, E. Lilley, P. Ferdinandy, and R. Schulz, "Best practices for blood collection and anaesthesia in mice: Selection, application and reporting," *British Journal of Pharmacology*, 2025.

[63] A. Vezyrakis, A. Guenther, and V. Mazza, "Effects of behavioural types on the problem-solving performance of wild house mice under controlled and semi-natural conditions," *Oikos*, p. e10787, 2025.

[64] T. Nevalainen, "Animal husbandry and experimental design," *ILAR Journal*, vol. 55, no. 3, pp. 392–398, 2014.

[65] J. A. Fontes, J. G. Barin, M. V. Talor, N. Stickel, J. Schaub, N. R. Rose, and D. Čiháková, "Complete freund's adjuvant induces experimental autoimmune myocarditis by enhancing il-6 production during initiation of the immune response," *Immunity, inflammation and disease*, vol. 5, no. 2, pp. 163–176, 2017.

[66] P. Wang, H. Jiang, J. Yao, G. He, T. Tao, and Z. Qin, "The effect of ponicidin on cfa-induced chronic inflammatory pain and its mechanism based on network pharmacology and molecular docking," *Frontiers in Medicine*, vol. 12, p. 1510271, 2025.

[67] C. A. N. Ismail, D. C. Tan, N. A. M. Khir, and N. Shafin, "A review on complete freund's adjuvant-induced arthritic rat model: factors leading to its success," *IIUM Medical Journal Malaysia*, vol. 21, no. 4, 2022.

[68] K. Mone, E. J. T. Garcia, F. Abdullatif, M. T. Rasquinha, M. Sur, M. Hanafy, D. K. Zinniel, S. Singh, R. Thomas, R. G. Barletta, T. Gebregiworgis, and J. Reddy, "Metabolic reprogramming in response to freund's adjuvants: Insights from serum metabolomics," *Microorganisms*, vol. 13, no. 3, p. 492, 2025.

[69] F. Forouzanfar, A. M. Pourbagher-Shahri, and A. M. Ahmadzadeh, "Rutin attenuates complete freund's adjuvant-induced inflammatory pain in rats," *Iranian Journal of Basic Medical Sciences*, vol. 28, no. 3, p. 332, 2025.

[70] Y. Ozdemir, K. Nakamoto, B. Boivin, D. Bullock, N. A. Andrews, R. González-Cano, and M. Costigan, "Quantification of stimulus-evoked tactile allodynia in free moving mice by the chainmail sensitivity test," *Frontiers in Pharmacology*, vol. 15, p. 1352464, 2024.

[71] M. U. Mazhar, S. Naz, T. Zulfiqar, J. Z. Khan, F. Hilal, S. Ghazanfar, and M. K. Tipu, "Bacillus subtilis (nmcc-path-14) ameliorates acute phase of arthritis via modulating nf-κb and nrf-2 signaling in mice model," *Inflammopharmacology*, pp. 1–15, 2025.

[72] J. N. Sharma, A. M. Samud, and M. Z. Asmawi, "Comparison between plethysmometer and micrometer methods to measure acute paw oedema for screening anti-inflammatory activity in mice," *InflammoPharmacology*, vol. 12, no. 1, pp. 89–94, 2004.

[73] A. G. Abbas, O. B. Ajiboye, P. A. Adeleke, A. M. Ajayi, O. Okubena, and S. Umukoro, "Polyphenol-rich sorghum bicolor supplement exhibits anti-nociceptive activity and protective effects against pathological changes associated with complete freund's adjuvant induced arthritis in rodents," *Pharmacological Research-Modern Chinese Medicine*, vol. 12, p. 100481, 2024.

[74] U. Aguwa, C. Eze, B. Obinwa, S. Okeke, S. Onwuelingo, D. Okonkwo, D. Ogbuokiri, A. Agulanna, I. Obiesie, and A. Umezulike, "Comparing the effect of methods of rat euthanasia on the brain of wistar rats: Cervical dislocation, chloroform inhalation, diethyl ether inhalation and formalin inhalation," *J Adv Med Med Res*, vol. 32, no. 17, pp. 8–1, 2020.

[75] M. Richner, S. B. Jager, P. Siupka, and C. B. Vaegter, "Hydraulic extrusion of the spinal cord and isolation of dorsal root ganglia in rodents," *Journal of visualized experiments: JoVE*, no. 119, p. 55226, 2017.

[76] X. Tao, Y. Huang, C. Wang, F. Chen, L. Yang, L. Ling, Z. Che, and X. Chen, "Recent developments in molecular docking technology applied in food science: a review," *International Journal of Food Science and Technology*, vol. 55, no. 1, pp. 33–45, 2019.

[77] R. M. de Angelo, D. S. de Sousa, A. P. da Silva, L. P. A. Chiari, A. B. F. da Silva, and K. M. Honorio, *Molecular Docking: State-of-the-Art Scoring Functions and Search Algorithms*. Cham: Springer Nature Switzerland, 2024, pp. 163–198.

[78] P. H. M. Torres, A. C. R. Sodero, P. Jofily, and F. P. Silva-Jr, "Key topics in molecular docking for drug design," *International Journal of Molecular Sciences*, vol. 20, no. 18, p. 4574, 2019.

[79] D. Seeliger and B. L. de Groot, "Ligand docking and binding site analysis with pymol and autodock/vina," *Journal of Computer-Aided Molecular Design*, vol. 24, no. 5, pp. 417–422, 2010.

[80] A. M. Vijesh, A. M. Isloor, S. Telkar, T. Arulmoli, and H.-K. Fun, "Molecular docking studies of some new imidazole derivatives for antimicrobial properties," *Arabian Journal of Chemistry*, vol. 6, no. 2, pp. 197–204, 2013.

[81] M. S. Valdés-Tresanco, M. E. Valdés-Tresanco, P. A. Valiente, and E. Moreno, "Amdock: a versatile graphical tool for assisting molecular docking with autodock vina and autodock4," *Biology Direct*, vol. 15, no. 1, p. 12, 2020.

[82] T. F. Vieira and S. F. Sousa, "Comparing autodock and vina in ligand/decoy discrimination for virtual screening," *Applied Sciences*, vol. 9, no. 21, p. 4538, 2019.

[83] J. E. Polli, "In vitro studies are sometimes better than conventional human pharmacokinetic in vivo studies in assessing bioequivalence of immediate-release solid oral dosage forms," *The AAPS Journal*, vol. 10, no. 2, pp. 289–299, 2008.

[84] C. Hirsch and S. Schildknecht, "In vitro research reproducibility: Keeping up high standards," *Frontiers in pharmacology*, vol. 10, p. 1484, 2019.

[85] G. Kumar and N. Singh, "Synthesis, anti-inflammatory and analgesic evaluation of thiazole/oxazole substituted benzothiazole derivatives," *Bioorganic Chemistry*, vol. 107, p. 104608, 2021.

[86] J. Chabry, S. Nicolas, J. Cazareth, E. Murris, A. Guyon, N. Glaichenhaus, C. Heurteaux, and A. Petit-Paitel, "Enriched environment decreases microglia and brain macrophages inflammatory phenotypes through adiponectin-dependent mechanisms: Relevance to depressive-like behavior," *Brain, behavior, and immunity*, vol. 50, pp. 275–287, 2015.

[87] S. Tariq, P. Kamboj, O. Alam, and M. Amir, "1, 2, 4-triazole-based benzothiazole/benzoxazole derivatives: Design, synthesis, p38α map kinase inhibition, anti-inflammatory activity and molecular docking studies," *Bioorganic chemistry*, vol. 81, pp. 630–641, 2018.